

# 1 **Root water uptake patterns are controlled by tree species** 2 **interactions and soil water variability**

3 Gökben Demir<sup>1</sup>, Andrew J. Guswa<sup>2</sup>, Janett Filipzik<sup>1</sup>, Johanna Clara Metzger<sup>1,3</sup>, Christine Römermann<sup>4,6</sup>,  
4 Anke Hildebrandt<sup>1,5,6</sup>

5 <sup>1</sup> Group of Terrestrial Ecohydrology, Institute of Geoscience, Friedrich Schiller University Jena, Jena,  
6 07749, Germany

7 <sup>2</sup> Picker Engineering Program, Smith College, Northampton, MA, 01063, USA

8 <sup>3</sup>Institute of Soil Science, University of Hamburg, Hamburg, 20146, Germany

9 <sup>4</sup>Plant Biodiversity, Institute of Ecology and Evolution, Friedrich Schiller University Jena, Jena, 07743,  
10 Germany

11 <sup>5</sup> Department of Computational Hydrosystems, Helmholtz Centre for Environmental Research – UFZ,  
12 Leipzig, 04318, Germany

13 <sup>6</sup>German Centre for Integrative Biodiversity Research (iDiv) Halle -Jena-Leipzig, Leipzig, 04103,  
14 Germany

15

16 Correspondence to: [goekben.demir@uni-jena.de](mailto:goekben.demir@uni-jena.de) and [anke.hildebrandt@ufz.de](mailto:anke.hildebrandt@ufz.de)

## 17 **Abstract**

18 Root water uptake depends on soil moisture which is primarily fed by throughfall in forests. Several biotic  
19 and abiotic elements shape the spatial distribution of throughfall. It is well documented that throughfall  
20 patterns result in reoccurring higher and lower water inputs at certain locations. However, how the spatial  
21 distribution of throughfall affects root water uptake patterns remains unresolved. Therefore, we  
22 investigate root water uptake patterns by considering spatial patterns of throughfall and soil water patterns  
23 in addition to soil and neighboring tree characteristics. In a beech-dominated mixed deciduous forest in a  
24 temperate climate, we conducted intensive throughfall sampling at locations paired with soil moisture  
25 sensors during the 2019 growing season. We employed a linear mixed-effects model to understand  
26 controlling factors for root water uptake patterns. Our results show that soil water patterns and interactions  
27 among neighbouring trees are the most significant factors regulating root water uptake patterns.  
28 Temporally stable throughfall patterns did not influence root water uptake patterns. Similarly, soil  
29 properties were unimportant for spatial patterns of root water uptake. We found that wetter locations

30 (rarely associated with throughfall hotspots) promoted greater root water uptake. Root water uptake in  
31 monitored soil layers also increased with neighbourhood species richness. Ultimately our findings suggest  
32 that complementarity mechanisms within the forest stand, in addition to soil water variability and  
33 availability, govern root water uptake patterns.

34

35 **Key words:** root water uptake, throughfall, soil water, spatial patterns, beech

## 36 **1) Introduction**

37 Root water uptake depends on soil moisture, which is replenished by precipitation. At the same time, the  
38 vegetation canopy intercepts and redirects precipitation into throughfall and stemflow, collectively  
39 referred to as below-canopy precipitation. Thus, even before soil water can be taken up by roots, it has  
40 already been influenced by the canopy.

41 Throughfall is typically the largest component of below canopy precipitation (Levia and Frost, 2006;  
42 Sadeghi et al., 2020). For instance, in temperate forests about 70% of above canopy precipitation ends up  
43 as throughfall (Levia and Frost, 2003; Sadeghi et al., 2020). Below-canopy precipitation is modified by  
44 several biotic and abiotic factors (Levia and Frost, 2006; Levia et al., 2011), including vegetation type,  
45 canopy architecture (Crockford and Richardson, 2000; Pypker et al., 2011; Levia et al., 2017), and forest  
46 structure (Rodrigues et al., 2022), meteorological elements such as wind speed (Staelens et al., 2008; Van  
47 Stan et al., 2011; Fan et al., 2015), precipitation intensity and event size (Dunkerley, 2014; Magliano et  
48 al., 2019; Zhang et al., 2016; Staelens et al., 2008). As a result, throughfall inherently varies across space  
49 and time. However, previous studies showed that the spatial distribution of throughfall persists over time  
50 (Keim et al., 2005; Staelens et al., 2006; Guswa and Spence, 2012; Carlyle-Moses et al., 2014; Metzger  
51 et al., 2017; Van Stan et al., 2020).

52 Throughfall patterns have been hypothesized to affect the spatial variation in water uptake (Bouten et al.,  
53 1992; Coenders-Gerrits et al., 2013) and soil moisture distribution (Raat et al., 2002; Blume et al., 2009;  
54 Zimmermann et al., 2009; Zehe et al., 2010; Bachmair et al., 2012; Rosenbaum et al., 2012; Zhang et al.,  
55 2016). Yet, empirical evidence is scarce. A decade ago Coenders-Gerrits et al., (2013) proposed that

56 throughfall patterns are translated into soil wetting dynamics with a model based on combined hillslope  
57 topographic and throughfall data collected in a beech-dominated catchment. However, in this model, the  
58 effect of throughfall patterns on soil moisture patterns rapidly ceased, and became more similar to the  
59 bedrock topography. Regarding the latter result, the model and reality differ, as the correlation between  
60 measured bedrock topography and soil moisture is low (Tromp-van Meerveld and McDonnell, 2006),  
61 which Coenders-Gerrits et al., (2013) attributed to root water uptake. Later, Metzger et al. (2017) showed  
62 through field observations that although throughfall spatial variation strongly increases shortly after  
63 rainfall it drops quickly again in the drained state, so the impact rapidly disappears. Later, Fischer-Bedtke  
64 et al., (2023) confirmed in the same field site that recurring throughfall patterns left a notable imprint on  
65 soil moisture response to rainfall yet the effect on absolute values of soil water content in drained state  
66 was rather weak. More recently, Zhu et al. (2021) observed that stable throughfall patterns were weakly  
67 related to the spatial distribution of soil moisture since this relationship was restricted only to relatively  
68 wet soil locations and throughfall hotspots. They also showed that throughfall patterns had weaker  
69 influence on the temporal dynamics of soil water content compared to soil bulk density and litter layer  
70 properties.

71 Taken together, several studies have searched for patterns of throughfall in soil moisture spatial variation.  
72 As comparatively weak relationships were found, some previous studies have suggested that root water  
73 uptake (Bouten et al., 1992; Schwärzel et al., 2009) could be the cause. Specifically, based on a one-  
74 dimensional soil-water model, Bouten et al. (1992) proposed that throughfall patterns alter and localize  
75 root water uptake as well as promote fast drainage. As a result, spatial variation in root water uptake could  
76 diminish the effect of throughfall patterns into spatio-temporal variation of soil water. However, other  
77 researchers suggested that other factors, such as soil properties (Metzger et al., 2017), preferential flow  
78 (Jost et al., 2004; Blume et al., 2009; Molina et al., 2019; Fischer-Bedtke et al., 2023) and litter layer  
79 processes (Raat et al., 2002) may be at the heart of the weak and short-term effects of throughfall patterns  
80 on soil moisture variability.

81 However, to the best of our knowledge, the feedback mechanism of throughfall patterns on root water  
82 uptake variation has not yet been investigated empirically. More common are studies related to soil water  
83 distribution. Soil water availability, which could potentially be enhanced by throughfall, affects root water

84 uptake patterns even more than root abundance (Kühnhammer et al., 2020; Guderle et al., 2018). On the  
85 flip side, root water uptake can amplify or homogenize soil water variability (Hupet and Vanclooster,  
86 2005; Teuling and Troch, 2005; Ivanov et al., 2010; Baroni et al., 2013; Martínez García et al., 2014).  
87 Moreover, variations in soil water content reflect on root water uptake (Hupet et al., 2002; Schume et al.,  
88 2004; Schwärzel et al., 2009; Guderle and Hildebrandt, 2015; Jackisch et al., 2020).

89 Next to water input, soil properties can alter root water uptake patterns (Nadezhdina et al., 2007; Kirchen  
90 et al., 2017). Also they control soil water redistribution (Grayson et al., 1997; Cosh et al., 2008; Jarecke  
91 et al., 2021) and water availability for root structures (Vereecken et al., 2007; Cai et al., 2018). For a given  
92 evaporative demand, water uptake at a particular location is a function of water transport resistance  
93 between root and soil in addition to the soil-water potential (Cardon and Letey, 1992; Shani and Dudley,  
94 1996; Lhomme, 1998). Both characteristics depend on local soil properties and soil water status, and the  
95 latter in turn is affected by the local water uptake rate.

96 Finally, plant individual and ecosystem processes affect uptake: Root networks can connect wetter and  
97 drier locations in a variety of ecosystems (e.g., Emerman and Dawson, 1996; Katul and Siqueira, 2010;  
98 Yu and D’Odorico, 2015; Priyadarshini et al., 2016; Hafner et al., 2017). In addition, tree size, age,  
99 neighboring tree species, and ecosystem structure affect the spatio-temporal variation in root water uptake  
100 (Volkman et al., 2016; Spanner et al., 2022; Kostner et al., 2002; Dawson, 1996; Brinkmann et al., 2019;  
101 Gaines et al., 2016; Silvertown et al., 2015; Guo et al., 2018; Brum et al., 2019; Krämer and Hölscher,  
102 2010).

103 Taken together, throughfall and soil water variability, soil properties, and root water uptake patterns form  
104 complex and intertwined interactions in the terrestrial hydrological cycle. It has not yet been shown  
105 empirically how root water uptake patterns are affected by throughfall and spatial distribution of soil  
106 water content. In line with previous modeling results (Bouten et al., 1992; Coenders-Gerrits et al., 2013)  
107 we hypothesize that throughfall hotspots enhance water availability at certain locations that elevate root  
108 water uptake. Further we investigate the role of soil water variation in combination with soil properties  
109 and neighboring tree characteristics on root water uptake patterns. We pose the following questions to  
110 test the main hypothesis and guide the investigation:

111 i) How do throughfall patterns influence root water uptake patterns?

- 112 ii) How does soil moisture and its variation, along with soil properties, control variation in root  
113 water uptake?
- 114 iii) What is the role of biotic factors, namely size, distance, number, and species richness of  
115 neighbouring trees on root water uptake patterns?

116 Here, we address these questions by employing a linear mixed effects model based on weekly throughfall  
117 sampling at locations paired with intensive soil moisture measurements in a beech-dominated unmanaged  
118 forest. We estimate root water uptake using a water balance method applied at soil moisture measurement  
119 point. This method dissects soil water flow and water uptake by exploring the differences in soil water  
120 content change per time between day and night (Guderle and Hildebrandt, 2015; Jackisch et al., 2020).  
121 While other methods exist, such as using isotopic tracers (Rothfuss and Javaux, 2017, Zarebanadkouki et  
122 al., 2013), daily fluctuations in soil water allow for estimating the spatial distribution of ecosystem  
123 evapotranspiration using standard measurements of soil water content (Guderle and Hildebrandt, 2016)  
124 without the need for additional infrastructure. In addition, we incorporate data on field capacity, bulk  
125 density, and neighboring tree characteristics namely size and species.

## 126 **2) Materials and Methods**

### 127 **2.1) Research Site and Field Sampling**

#### 128 **2.1.1) Research Site**

129 The research site is located in the forested upper hill region of the Hainich low mountain range in  
130 Thuringia, Germany, as a part of the Hainich Critical Zone Exploratory (CZE) (Küsel et al., 2016). The  
131 altitude in the research site ranges from 362 m to 368 m a.s.l. Mean annual air temperature varies between  
132 7.5 and 9.5 °C, and the mean annual precipitation ranges from less than 600 to 1000 mm in the CZE  
133 (Küsel et al., 2016).

134 In the study area, thin-bedded alternations of limestones and marlstones of carbonate rock (Middle  
135 Triassic) form the bedrock overlain by a shallow Pleistocene loess layer with cambisols and luvisols as  
136 dominant soil types (IUSS Working Group, 2006; Metzger et al., 2021). The median soil depth above the

137 weathered bedrock is 37 cm, with soil depths ranging from 15 cm to a maximum depth of 87 cm (Metzger  
138 et al., 2017).

139 In 2019, the tree community in the research site consisted of 574 individuals of various ages (diameter at  
140 breast height  $\geq 5$ cm). The dominant species is European beech (*Fagus sylvatica* L.), which makes up 70%  
141 of the tree community, followed by sycamore maple (*Acer pseudoplatanus* L.) with 21 %, and European  
142 ash (*Fraxinus excelsior* L.) with 4%. These dominant species are accompanied by Large-leaved linden  
143 (*Tilia platyphyllos* Scop.), European hornbeam (*Carpinus betulus* L.), Norway maple (*Acer platanoides*  
144 L.), Scots elm (*Ulmus glabra* L.), and Wild service tree (*Sorbus torminalis* (L.) Crantz). The stand has a  
145 total basal area of 40 m<sup>2</sup> ha<sup>-1</sup> and has been unmanaged since 1997 (Kohlhepp et al., 2017).

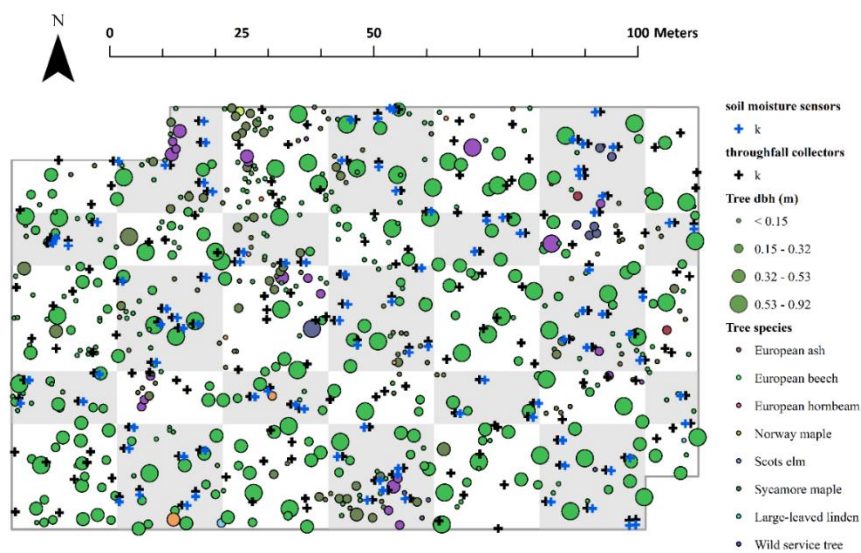
### 146 **2.1.2) Soil moisture monitoring and soil properties**

147 The forest site (1 ha) was equipped with a soil moisture monitoring network (SoilNet; Bogena et al., 2010)  
148 consisting of SMT100 frequency domain sensors (Treuebner GmbH, Neustadt, Germany). Metzger et al.  
149 (2017) first described the soil moisture monitoring setup. Briefly, the observation platform (Figure 1) was  
150 divided into 100 subplots (10 m  $\times$  10 m), and 49 subplots were equipped with soil moisture sensors at  
151 two random measuring points each, for a total of 98 locations. At each measuring point, sensors were  
152 placed at two different depths, 7.5 cm (top sensors) and 27.5 cm (bottom sensors). The soil moisture  
153 network is maintained through a regular bi-weekly routine to avoid potential failures such as depleted  
154 sensors batteries, hardware problems, etc.

155 Undisturbed soil samples were collected during the sensor installation in 2014 and 2015 to estimate bulk  
156 density and water content at field capacity. In addition, we collected additional disturbed soil samples (n  
157 = 40) near sensor locations in 2019. Bulk density was determined from oven-dried (24h, 105°C) soil mass  
158 weight and water content at field capacity by applying 60 hPa pressure to the saturated undisturbed sample  
159 for 72 h.

160 Soil properties vary slightly from top to subsoil at the research site. While silty loam is the dominant soil  
161 texture in both layers, the clay content is higher in the subsoil (Metzger et al., 2021). The median  
162 volumetric water content at field capacity is 44% in the topsoil and 42% in the subsoil. Moreover, the  
163 water content at field capacity varies from 27% to 60% and from 31% to 62% in the topsoil and subsoil,

164 respectively. The average bulk density ( $d_{\text{bulk}}$ ) of the topsoil is  $1.16 \text{ g cm}^{-3}$ , with a range of  $0.73$  to  $1.5 \text{ g}$   
165  $\text{cm}^{-3}$ . In the subsoil, the average bulk density ( $d_{\text{bulk}}$ ) is slightly higher at  $1.37 \text{ g cm}^{-3}$  but has a similar range  
166 ( $0.7 - 1.6 \text{ g cm}^{-3}$ ) (See supplement for details).



167  
168 **Figure 1** (above) The photo of the site. (below) the field monitoring setup of stratified randomly distributed throughfall  
169 collectors and soil moisture sensors together with the trees which are sized according to the diameter at breast height (dbh)

170 and coloured according to the species. Throughfall collectors are paired with soil moisture sensors at 98 locations (n=182) in  
171 the grey shaded subplots. White coloured subplots are equipped with only throughfall collectors.

### 172 **2.1.3) Gross precipitation and throughfall sampling**

173 Five gross precipitation funnels were placed 1.5 m above ground level in an adjacent open grassland (ca.  
174 250 m distance to the research site). As described in Metzger et al. (2017) and Demir et al. (2022), the  
175 precipitation funnels were made of a circular plastic funnel (12 cm in diameter) and sampling bottle (2 L  
176 in volume), and ping pong balls were placed in the funnel orifice to prevent evaporation losses.

177 During the early growing season of 2019, we placed throughfall collectors in soil moisture monitoring  
178 subplots at 98 locations. We paired these throughfall collectors with the soil moisture sensors by placing  
179 them within 1 m of each other. The paired collectors were placed down-slope to avoid interference with  
180 soil moisture measurements. For the rest of the research site, in 51 other subplots, we adopted a separate  
181 independent stratified random design from Metzger et al. (2017). Briefly, we placed two throughfall  
182 collectors in each subplot that was not equipped with soil moisture sensors. All throughfall collectors  
183 were placed roughly 37 cm above the ground.

184 We conducted weekly manual measurement of throughfall and gross precipitation during the 2019  
185 growing season (April to August). Sampling was conducted on rain free days only. Thus, the sampling  
186 interval ranged between six and eight days.

187 We used the paired throughfall collectors (n = 98) to identify the drivers of root water uptake patterns, as  
188 we derived root water uptake values based on soil water content measurements (see below). However, we  
189 used all randomly placed throughfall collectors (n = 200) to describe the spatio-temporal variation of  
190 throughfall within the research site.

### 191 **2.2) Estimation of potential evapotranspiration**

192 We calculated the daily potential evapotranspiration by applying the concept of thermodynamic limits of  
193 convection (Kleidon and Renner, 2013; Kleidon et al., 2014):

$$194 E_{\text{pot}} = \frac{1}{\lambda} \frac{s}{s + \gamma} \frac{R_{sn}}{2} \quad (1)$$

195 Where  $R_{sn}$  is absorbed solar radiation ( $\text{W m}^{-2}$ ),  $\lambda$  is the latent heat of vaporization ( $2.5 \times 10^6 \text{ J kg}^{-1}$ ),  $\gamma$  is  
196 the psychrometric constant ( $65 \text{ PaK}^{-1}$ ), and  $s$  is the slope of the saturation vapor pressure curve ( $\text{PaK}^{-1}$ ).



197 Here, we acquired solar radiation, air temperature, and precipitation data for the throughfall sampling  
198 period from a nearby weather station ("Reckenbuel") which is located approximately 1.4 km northeast of  
199 the research site and provides data in 10 minutes intervals. The site-specific albedo for the summer period  
200 was adopted from Otto et al. (2014).

201 We used the precipitation data measured at the weather station to define rain events and dry periods, as  
202 described below.

## 203 **2.3) Data analysis**

### 204 **2.3.1) Quality control of soil water content data**

205 We systematically reviewed the six-minute soil water content data for quality control in two steps: 1)  
206 identification of problems (such as jumps to extremely low and high values, duplicated time stamps of  
207 different values, long discontinuities in the measurements, and lack of temporal variation in the time series  
208 despite rain events), 2) classification and removal of detected outliers and irregularities. We visually  
209 identified and removed unrealistic measurements such as extremely low ( $< 5$  vol-%) and high values far  
210 beyond the field capacity ( $> 75$  vol-%) and long plateaus of repeated values despite rain events. We also  
211 excluded any time series that exhibited long-term discontinuities that prevented us from calculating root  
212 water uptake. During the visual inspection, we eliminated values with duplicated time stamps that violated  
213 the actual temporal trend. Next, we scanned the data using the Hampel filter function of the 'pracma' R  
214 package (Borchers, 2021) with customized moving window length and Pearson's rule threshold value  
215 (Pearson, 1999) to flag possible outliers.

216 Despite regular maintenance, many sensors failed to provide data that met the quality criteria during the  
217 growing season (March-August) in 2019. Only 56 sensor locations (out of 98) provided data from both  
218 top and bottom sensors that met the qualification criteria described above with varying date intervals  
219 throughout the growing season. Of these, only 34 sensor locations were used to estimate root water uptake  
220 as they simultaneously provided data from both top and bottom sensors within the dry periods.

### 221 **2.3.2) Soil water calculation**

222 We estimated soil water ( $S$ ) at measurement locations for the monitored soil layer based on volumetric  
223 soil water content measured by top and bottom sensors.

$$224 S_{i,d} = \sum z_t \theta_{i,d}^t + z_b \theta_{i,d}^b \quad (2)$$

225 We similarly integrated the soil water at field capacity ( $S_{FC,i}$ )

$$226 S_{FC,i} = \sum z_t \theta_{FC,i}^t + z_b \theta_{FC,i}^b \quad (3)$$

227 where  $z_t$  is the depth of the soil column monitored by the top sensor and  $z_b$  is the depth of soil represented  
228 by the bottom sensor, and  $\theta_{i,d}$  is volumetric soil water content at location  $i$  on date  $d$ , and  $\theta_{FC,i}$  the soil  
229 water content at the field capacity.

230 We calculated bulk density at the sensors' locations for the monitored soil layer.

$$231 \overline{d}_{bulk,i} = \frac{\sum z_t d_{bulk,i}^t + z_b d_{bulk,i}^b}{\sum z_t + z_b} \quad (4)$$

232 where  $d_{bulk,i}^t$  and  $d_{bulk,i}^b$  are the bulk density of the topsoil and subsoil, respectively, at location  $i$ .

### 233 **2.3.3) Descriptive Statistics**

234 We calculated the coefficient of quartile variation (CQV) and the interquartile range to describe spatial  
235 variation of throughfall, volumetric soil water content, and root water uptake. Also, we estimated octile  
236 skewness ( $OS_8$ ) of throughfall based on the first and seventh octile.

$$237 CQV = \frac{Q_3 - Q_1}{Q_3 + Q_1} \quad (5)$$

$$238 OS_8 = \frac{(Q_7 - median) - (median - Q_1)}{Q_7 - Q_1} \quad (6)$$

239 We characterized spatial patterns of daily root water uptake ( $E_t$ ) by calculating the spatial deviation from  
240 the mean ( $\delta E_{t,i,d}$ , Equation 7) (Vachaud et al., 1985).

$$241 \delta E_{t,i,d} = \frac{E_{t,i,d} - \overline{E}_{t,d}}{\overline{E}_{t,d}} \quad (7)$$

242 where  $E_{t,i,d}$  is daily root water uptake estimated at  $i$  sensor location on date  $d$  and  $\overline{E}_{t,d}$  is spatial average  
243 of daily root water uptake on date  $d$ .

244 Similarly, we calculated the spatial deviation of soil water and throughfall to identify their spatial patterns.

## 245 **2.4) Root water uptake estimation**

246 We estimated root water uptake using the multi-step, multi-layer regression method (MSML), which is a  
247 water-balance method and derives evapotranspiration from diurnal differences in soil water content  
248 (Guderle and Hildebrandt, 2015; Guderle et al., 2018). This approach does not require prior information  
249 on root structure but relies on high temporal and spatial resolution data on multiple soil layers. Previous  
250 studies using additional measurements such as sap-flow and lysimeters demonstrated that the MSML  
251 method successfully estimates transpiration in both forest and grassland ecosystems (Guderle et al., 2018;  
252 Jackisch et al., 2020).

253 As described in Guderle and Hildebrandt (2015), the MSML derives root water uptake from distinct  
254 differences in the day and night portions of soil moisture time series. The main assumption is that, in the  
255 absence of rainfall-driven rapid vertical soil water flow, evapotranspiration occurs only during the day,  
256 while soil water flow occurs both during the day and at night. As a result, soil moisture time series reflect  
257 a distinct day/night signal under dry weather conditions.

258 In applying this method to our study, we first excluded potential periods of fast vertical flow periods from  
259 the time series due to previous rainfall events and identified periods for estimating daily root water uptake.  
260 We considered an 8 h buffer period to include canopy dripping and 48 h for the cessation of rainfall  
261 influence on soil water. Thus, a total of 56 h was the time interval used to define the start of the water  
262 uptake estimation period. The period when the root water uptake is estimated is hereafter referred to as  
263 the dry period.

264 Next, we split each soil moisture time series into a day (transpiration active period) and a night branch,  
265 as explained by Guderle and Hildebrandt (2015). We defined the transpiration period (starts 2 h after  
266 sunrise and ends 2 h before sunset) based on local sunrise and sunset time. Sunrise and sunset times were  
267 obtained from the R package 'suncal' (Thieurmél and Elmarhraoui, 2022). We fit linear models to each  
268 split branch of the time series and derived the slopes. The difference between the slope of the day branch  
269 ( $m_{tot}$ ) and the average slope of the antecedent and preceding night ( $\overline{m_{flow,i}}$ ) gives the rate of water uptake.  
270 Thus, we estimated daily evapotranspiration at each soil water content location  $i$  (Equation 8, 9) by  
271 accounting for soil layer thickness and slope difference-

272

$$E_{t,msml,i}^{t,b} = (m_{tot,i}^{t,b} - \overline{m_{flow,t}^{t,b}}) d_{z,i}^{t,b} \quad (8)$$

$$E_{t,i} = \sum(E_{t,msml,i}^t + E_{t,msml,i}^b) \quad (9)$$

275

## 276 **2.5) Linear Mixed Effects Model**

277 We employed a linear mixed effects model to investigate the driving factors for root water uptake patterns.

278 A linear mixed effects model is a multivariate statistical tool that describes the relationship between a  
 279 dependent variable and explanatory variables (fixed effects) while controlling for dependencies in the  
 280 data that may arise due to repeated sampling with certain designs (random effects). Fixed effects are  
 281 informative, repeatable levels of explanatory and quantified variables that can influence the mean of the  
 282 dependent variable, and they can be tested. In addition, in a linear mixed-effects model, how the  
 283 relationship between the dependent variable and one predictor depends on the level of another predictor  
 284 can be represented via interaction term.

285 Random factors are uninformative levels of predictor variables but can explain parts of the residual of the  
 286 fixed effects model by calculating different intercepts for different category levels. They are included in  
 287 mixed effects models to account for qualitative information from repeated sampling with respect to  
 288 individuals, time stamps, or treatments. Here, sensor location and dry period, i.e. date, are taken as random  
 289 effects.

290 For the model, we used only paired throughfall and soil moisture measurement locations where both top  
 291 and bottom sensors provided data during the dry periods. All considered explanatory drivers, which are  
 292 included as fixed factors in the model, are listed in Table 1. These factors include abiotic and biotic  
 293 variables that possibly influence relative local root water uptake: They are daily spatial average soil water  
 294 storage, the spatial deviation of soil water from the mean, soil water at field capacity and bulk density of  
 295 the monitored soil layer.

296 To account for spatial variability in throughfall, we calculated the spatial deviation from the mean by  
 297 using Equation 7. Here we considered this variable at a two-different time scales: the sampling week(s)  
 298 prior to root water uptake estimation, and over the entire throughfall sampling period.

299 Further, as biotic factors, we included number of trees, and number of species within a 5 m radius of each  
300 soil moisture location, and inverse-distance-weighted basal area (BA) within 5 m radius of each soil  
301 moisture location, calculated as follows:

$$302 \quad BA_i = \frac{\sum_{R=1}^R W_R A_{tree}}{A} \quad (10)$$

$$303 \quad \text{with } W_R = \frac{(x_i - x_R)^2}{\sum_R (x_i - x_R)^2} \quad (11)$$

304 where  $i$  is the soil moisture sensor located at  $x_i$ ,  $R$  is the tree index located at  $x_R$ , and  $A_{tree}$  is the individual  
305 basal area of the corresponding tree,  $A$  is the area around the soil moisture sensor  $i$  with 5 m in radius.

306 Even though our research plot is a beech-dominated forest, in some spots, two to four species were present  
307 within a 5 m radius of the soil moisture sensors.

308 We also included interaction terms (Table 1) as fixed factors in the model to capture complex and non-  
309 linear relationships among the biotic and abiotic factors.

310 We conducted all analyses with the R statistical software (R Core Team, 2022) and used the *lmer* function  
311 in the 'lme4' package (Bates et al., 2015) for the model development. We visually checked the model  
312 assumptions using the 'check\_model' function of the 'performance' package (Lüdtke et al., 2021).

313 In addition, we calculated both conditional and marginal  $R^2$  of the model with the 'MuMIn' package  
314 (Bartoń, 2020). While the conditional  $R^2$  includes the variance of the entire model, the marginal  $R^2$   
315 subsumes only the fixed effects (Bartoń, 2020). Before fitting the linear mixed effects model, we tested  
316 for co-linearity of the considered variables and scaled the data with a Z-transformation by using the 'scale'  
317 function in base R (R Core Team, 2022), which allowed us to evaluate the individual effect of fixed effects  
318 by comparing slopes and significance levels.

319 We developed the optimal model by applying a systematic model selection procedure based on Akaike's  
320 Information Criterion (AIC) comparison in combination with the examination of the factors. Model  
321 selection began with the beyond-optimal model, which included all possible fixed and random effects.  
322 We stepwise evaluated each fixed effect based on its respective significance ( $p$  value comparison) by  
323 fitting the model the maximum likelihood (ML) to be able to compare AIC values (Zuur et al., 2009). In  
324 each step, starting with interaction terms, we identified the least significant effect and formulated a model  
325 without it. We compared the AIC values of the model before and after removing the effect, discarding it

326 in case the AIC was unaffected or decreased. We followed the procedure with the next equally detected  
 327 effect, and repeated it until only significant fixed effects remained, and the model with the lowest AIC  
 328 (the optimal model) was obtained.

329 As a final step, the best model was refitted with restricted maximum likelihood (REML) (Zuur et al.,  
 330 2009).

331 **Table 1** List of fixed and random factors considered for estimating the root water uptake patterns through linear mixed effects  
 332 model. Interaction is shown with ‘x’.

<b>Fixed Factors</b>	
<b>Single Factors</b>	<b>Interaction Factors</b>
Spatial average of soil water storage in the monitored soil layer ( $\bar{S}$ )	$\bar{S} \times S_{FC}$
Spatial deviation of soil water storage from the mean ( $\delta S$ )	$\delta S \times S_{FC}$
Field capacity of the monitored soil layer ( $S_{FC}$ )	$\delta S \times BA$
Bulk density capacity of the monitored soil layer ( $d_{bulk}$ )	$\bar{S} \times BA$
Spatial deviation of throughfall of events measured in sampling week previous to the corresponding dry period ( $\delta P_{TF_{last\ ev.}}$ )	$\delta S \times n_{tree}$
The median of spatial deviation of throughfall measured within the whole sampling period ( $\widetilde{\delta P_{TF}}$ )	$\bar{S} \times n_{tree}$
Number of trees ( $n_{tree}$ )	$\delta P_{TF_{last\ ev.}} \times S_{FC}$
Basal area (BA)	$\delta P_{TF_{temp.\ stable.}} \times S_{FC}$
Number of species ( $n_{sp,tree}$ )	$\delta P_{TF_{last\ ev.}} \times d_{bulk}$
	$\delta P_{TF_{temp.\ stable.}} \times d_{bulk}$
	$n_{sp,tree} \times WA_{int}$
<b>Random factors</b>	
Soil moisture sensor location	
Dry period	

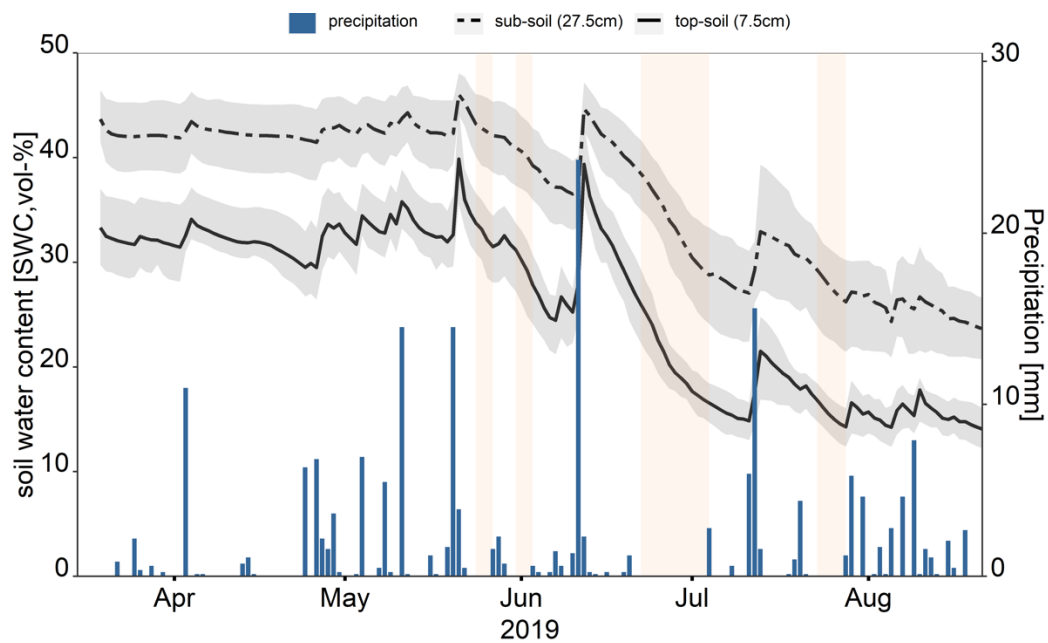
### 3) Results

#### 3.1) Spatio-temporal distribution of throughfall and soil water content

In 12 out of the 16 sampling weeks, the weekly gross precipitation was more than half of the total potential evapotranspiration. Table 2 shows the distribution of throughfall sampled in 2019 (April-August) at 200 collectors and the 98 collectors that were paired with soil moisture sensors. Weekly throughfall increased with an increase in rain. The coefficient of quartile variation (CQV) of throughfall was generally lower for larger cumulative weekly rains. On average, the collectors paired with soil-moisture sensors received similar amounts of throughfall to all collectors (Table 2). The CQV of data from the paired collectors ranged from 0.27 to 0.6, which is similar to the CQV of throughfall sampled at all collectors. The octile skew ( $OS_8$ ) of paired and all collectors was also similar.

As the growing season progressed in 2019, the average soil water content decreased in both the topsoil and subsoil. In April and early May, the average volumetric soil water content in the topsoil was above 30%, and dropped to below 10% by the end of August. In the subsoil, the volumetric soil water content similarly declined from above 40 % to below 20 % over the sampling period (Figure 2). On average, soil water changed from 52.5mm to 17.5 mm in the topsoil and from 80 mm to 40mm in the subsoil.

We derived root water uptake for four periods (a total of 19 days) under different soil wetness conditions that captured the seasonal variation of soil water content, including late spring when the soil water content was higher and drier periods during the summer following re-wetted soil conditions with late summer rains. As listed in Table 3 and shown in Figure 2, two periods were in late May and early June, and each lasted two days. The third period began in late June and lasted 11 days; the last was four days in late July. From the start of the first dry period to the end of the last, the average soil water content declined from 33 to 15 % in the topsoil and from 43 to 27% in the subsoil. Table 3 shows that within the dry periods, the coefficient of quartile variation (CQV) of soil water content was between 0.09 -0.14 and 0.08 to 0.16 in the topsoil and subsoil, respectively. During the dry periods, the spatial heterogeneity of soil water content in the subsoil increased systematically. In contrast, the spatial variation of soil water content in the topsoil was not correlated with soil dryness.



359

360

361

362

363

**Figure 2** Soil moisture temporal variation in top and subsoil together with the daily precipitation measured at the nearby Reckenbühl station (approximately 1.4 km to the Northeast). The solid and dashed lines are spatial mean of soil water content estimated based on top (7.5 cm) and bottom (27.5 cm) sensors, and grey shaded areas show first and third quartiles. The reddish shaded areas show defined dry periods within the throughfall sampling when root water uptake could be estimated.



**Table 2** Cumulative potential evapotranspiration in mm ( $E_{\text{pot,cum}}$ ), gross precipitation ( $P_g$ ), the ratio of total precipitation to the potential evapotranspiration, spatial mean of throughfall based on all collectors ( $\overline{P_{TF}}$ ), spatial mean of throughfall based paired collectors ( $\overline{P_{TF}}$ ) in mm, interquartile range (IQR), coefficient of quartile variation (CQV) and octile skewness ( $OS_8$ ) of both all and paired throughfall collectors during the sampling week. The values are ordered according to the cumulated gross precipitation size.

Date	$E_{\text{pot,cum}}$	$P_g$	$P_g/E_{\text{pot}}$	$\overline{P_{TF}}$	$\frac{IQR}{\overline{P_{TF}}}$	$\frac{CQV}{\overline{P_{TF}}}$	$\frac{OS_8}{\overline{P_{TF}}}$	$\overline{P_{TF,paired}}$	$\frac{IQR}{\overline{P_{TF,paired}}}$	$\frac{CQV}{\overline{P_{TF,paired}}}$	$\frac{OS_8}{\overline{P_{TF,paired}}}$
04-06-2019	13.55	0.76	0.06	0.35	0.18	0.25	0.46	0.34	0.16	0.24	0.49
26-06-2019	20.87	1.73	0.08	0.97	0.44	0.24	0.16	0.98	0.53	0.27	0.27
17-04-2019	5.62	2.42	0.43	1.72	0.27	0.08	0.23	1.72	0.33	0.09	0.09
18-06-2019	9.46	4.00	0.42	2.58	0.62	0.12	-0.03	2.57	0.53	0.10	-0.08
29-05-2019	10.15	6.27	0.62	3.77	1.24	0.17	-0.52	3.63	1.50	0.21	-0.42
24-07-2019	13.52	7.80	0.58	4.61	1.06	0.12	-0.34	4.48	0.88	0.10	-0.63
21-08-2019	8.94	8.54	0.96	5.19	1.06	0.10	-0.47	5.17	0.97	0.10	-0.44
30-07-2019	12.68	10.73	0.85	7.81	2.25	0.15	-1.51	7.58	2.28	0.15	-1.17
07-05-2019	6.65	12.56	1.89	9.21	1.33	0.07	-0.75	9.21	1.99	0.11	-1.05
14-08-2019	8.51	13.79	1.62	11.19	2.65	0.12	-1.40	10.99	2.98	0.13	-1.13
08-08-2019	13.91	23.87	1.72	16.60	2.65	0.08	-1.10	16.52	2.65	0.08	-1.17
30-04-2019	5.93	24.47	4.13	18.44	3.09	0.08	-1.63	18.30	2.65	0.07	-1.23
17-07-2019	8.28	29.27	3.54	24.22	3.54	0.07	-2.08	24.39	3.54	0.07	-2.59
15-05-2019	7.42	29.53	3.98	22.10	3.54	0.08	-2.11	22.21	3.54	0.08	-2.11
22-05-2019	6.74	41.82	6.20	30.94	3.54	0.06	-3.04	30.54	3.54	0.06	-3.46
13-06-2019	14.47	71.84	4.96	57.77	8.51	0.07	-5.82	57.99	7.29	0.06	-6.52

365 **Table 3** The spatial average of daily volumetric soil water content ( $\overline{\theta_{\text{top-soil}}}$ , vol-%) in topsoil (0-17.5 cm), and ( $\overline{\theta_{\text{subsoil}}}$ , vol-%)  
 366 in subsoil (17.5 – 37.5 cm) during the defined dry periods. The inter quartile range (IQR), and coefficient of quartile variation  
 367 (CQV) of daily volumetric soil water content in both layers during the dry periods.

Date	$\overline{\theta_{\text{top-soil}}}$ (vol-%)	IQR $\theta_{\text{top-soil}}$ (vol-%)	CQV $\theta_{\text{top-soil}}$ (vol-%)	$\overline{\theta_{\text{sub-soil}}}$ (vol-%)	IQR $\theta_{\text{subsoil}}$ (vol-%)	CQV $\theta_{\text{subsoil}}$ (vol-%)	Dry Period
25-05-2019	33.17	5.72	0.09	42.82	6.72	0.08	1
26-05-2019	32.12	6.62	0.10	42.46	6.67	0.08	1
01-06-2019	30.23	6.87	0.12	40.61	6.9	0.09	2
02-06-2019	29.22	7.23	0.13	40.11	6.85	0.09	2
23-06-2019	25.01	6.69	0.14	37.80	6.38	0.08	3
24-06-2019	24.04	6.45	0.14	36.94	6.22	0.08	3
25-06-2019	22.52	5.43	0.12	36.13	6.54	0.09	3
26-06-2019	21.48	5.07	0.12	35.24	6.71	0.10	3
27-06-2019	20.20	4.25	0.11	33.98	7.75	0.12	3
28-06-2019	19.45	3.85	0.10	33.31	8.08	0.12	3
29-06-2019	18.98	3.83	0.10	32.36	8.05	0.12	3
30-06-2019	18.44	3.52	0.09	31.37	8.15	0.13	3
01-07-2019	17.67	3.62	0.10	30.45	8.18	0.13	3
02-07-2019	17.29	4.18	0.12	29.84	8.87	0.15	3
03-07-2019	16.89	3.72	0.11	29.26	8.98	0.15	3
24-07-2019	16.15	3.48	0.11	28.56	8.7	0.16	4
25-07-2019	15.51	3.47	0.11	27.85	8.67	0.16	4
26-07-2019	14.98	3.57	0.12	27.21	8.49	0.16	4
27-07-2019	14.57	3.65	0.13	26.65	8.63	0.16	4

368

### 369 **3.2) Soil water storage, potential evapotranspiration, and root water uptake**

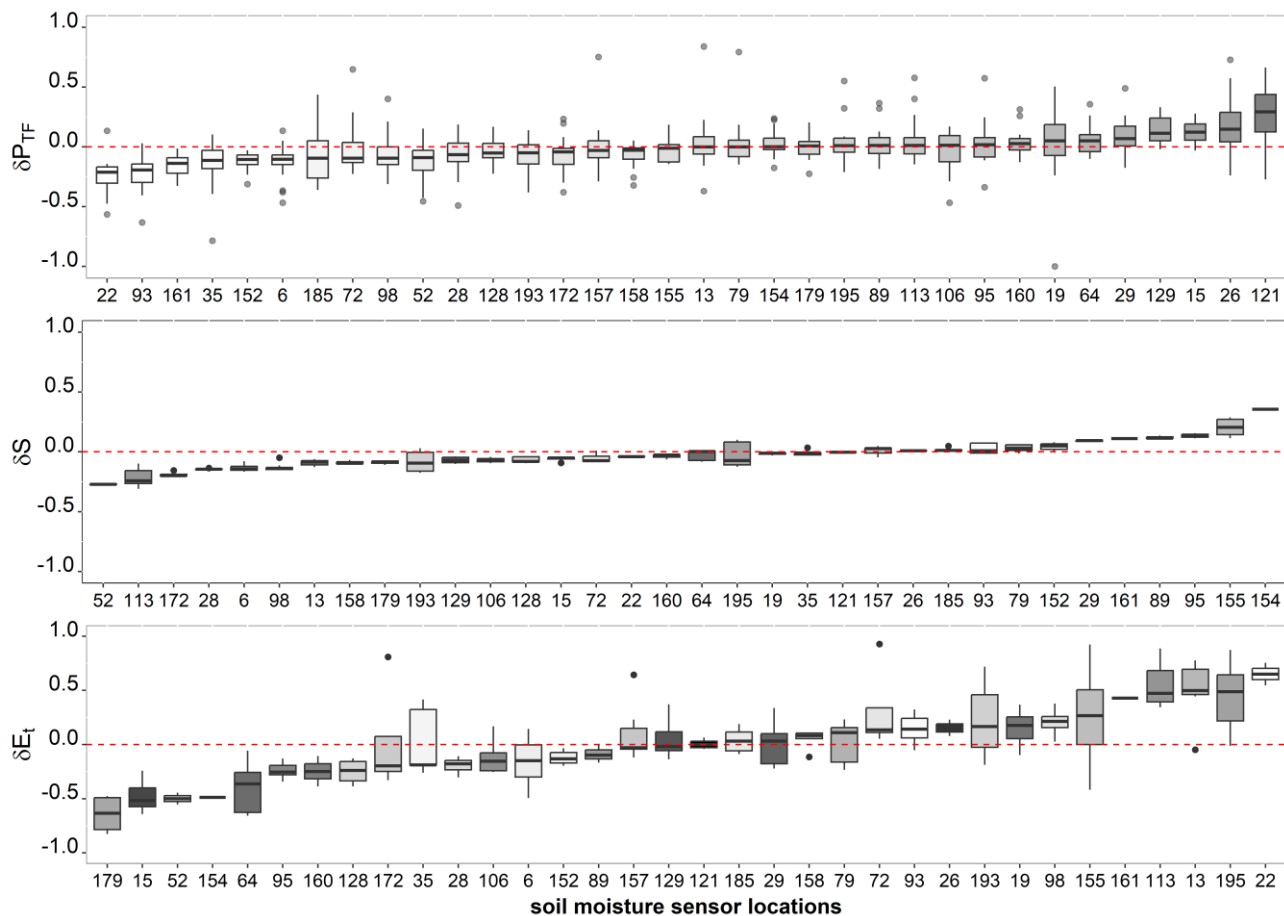
370 The integrated field capacity of the monitored soil depth was 160 mm on average at the research site.  
 371 Table 4 shows that soil water was much lower than the field capacity during the dry periods, and the mean  
 372 soil water storage dropped below 42 mm in late July. In addition, Table 4 demonstrates that the average  
 373 root water uptake ( $\overline{E}_t$ ) ranged from 0.94 mm d<sup>-1</sup> to 3 mm d<sup>-1</sup> while potential evapotranspiration ( $E_{\text{pot}}$ )  
 374 ranged from 1.75 mm d<sup>-1</sup> to 3.12 mm d<sup>-1</sup>. The discrepancy between average root water uptake and the  
 375 potential evapotranspiration increased as soil water decreased, especially during the longest dry period  
 376 (Table 4). Root water uptake showed greater spatial variation than water input and soil wetness. The  
 377 coefficient of quartile variation (CQV) of root water uptake ranged from 0.15 to 0.28, which was higher  
 378 than the CQV of throughfall and volumetric soil water content in both soil layers.

379 **Table 4** The daily average air temperature ( $T_{\text{air}}$ , °C), potential evapotranspiration ( $E_{\text{pot}}$ , mm), mean soil water storage ( $\bar{S}$ , mm)  
 380 in monitored soil layer (0 - 37.5 cm), and spatial mean of daily root water uptake ( $\bar{E}_t$ , mm) based on all soil moisture sensors,  
 381 and the ratio of the root water uptake to the potential evapotranspiration together with and standard deviation (SD) and  
 382 coefficient of quartile variation (CQV) of the daily root water uptake during the defined dry periods

Date	$T_{\text{air}}$ (°C)	$E_{\text{pot}}$ (mm)	$\bar{S}$ (mm)	$\bar{E}_t$ (mm)	$\bar{E}_t / E_{\text{pot}}$ (%)	SD $\bar{E}_t$	CQV $\bar{E}_t$	Dry Period
25-05-2019	12.74	1.80	71.94	1.09	60.56	0.38	0.28	1
26-05-2019	14.43	1.90	70.57	1.30	68.42	0.48	0.25	1
01-06-2019	18.42	2.59	67.16	2.26	87.26	0.98	0.27	2
02-06-2019	21.38	2.77	65.79	2.50	90.25	1.12	0.18	2
23-06-2019	19.45	2.79	59.81	2.83	101.43	0.90	0.19	3
24-06-2019	20.22	2.82	58.16	2.62	92.91	0.76	0.17	3
25-06-2019	22.52	2.89	55.96	2.67	92.39	0.78	0.16	3
26-06-2019	25.73	2.96	54.13	3.00	101.35	0.88	0.15	3
27-06-2019	18.83	2.75	51.91	2.28	82.91	0.55	0.16	3
28-06-2019	16.07	2.58	50.55	1.53	59.30	0.40	0.20	3
29-06-2019	19.59	2.85	49.55	2.11	74.04	0.60	0.20	3
30-06-2019	25.54	3.12	48.26	2.57	82.37	0.86	0.18	3
01-07-2019	20.63	2.30	46.69	1.59	69.13	0.53	0.18	3
02-07-2019	14.88	1.75	45.81	1.08	61.71	0.42	0.24	3
03-07-2019	13.77	1.91	44.95	0.94	49.21	0.30	0.23	3
24-07-2019	24.39	2.76	43.61	1.88	68.12	0.64	0.19	4
25-07-2019	25.33	2.82	42.31	1.77	62.77	0.60	0.24	4
2019-07-26	23.27	2.64	41.18	1.40	53.03	0.55	0.18	4
2019-07-27	21.29	2.68	40.23	1.21	45.15	0.47	0.19	4

### 383 3.3) Soil water, throughfall, and root water uptake patterns

384 At soil moisture measurement points where daily root water uptake was determined ( $n = 34$ ), we  
 385 calculated the spatial deviation from the median of throughfall, soil water storage, and root water uptake  
 386 to illustrate the spatial patterns. Figure 3 shows that some locations received repeatedly less (or more)  
 387 throughfall than average ( $\delta P_{TF} < 0$ ), some locations were repeatedly wetter or drier ( $\delta S < 0$ ), and some  
 388 places regularly had lower or higher root water uptake ( $\delta E_t$ ) throughout the sampling period. However,  
 389 these locations were not related to each other. In fact, Figure 3 demonstrates that neither throughfall nor  
 390 soil water patterns are directly correlated with the root water uptake patterns. For example, the locations  
 391 with higher water uptake were not coupled with elevated throughfall input (locations coloured dark) or  
 392 higher soil water storage. In addition, soil water storage patterns were not correlated with throughfall  
 393 patterns.



394

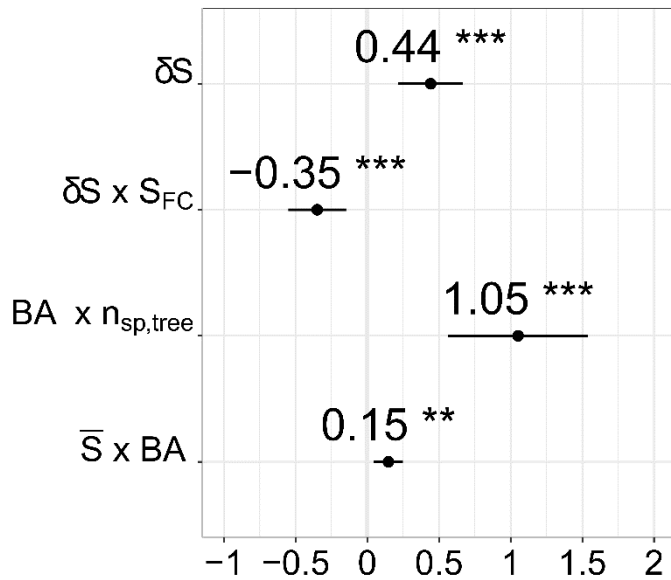
395 **Figure 3** Temporal stability of throughfall patterns which is estimated by the spatial deviation from the mean ( $\delta P_{TF}$ ) throughout  
 396 the sampling period in 2019 (April-August), soil water ( $\delta S$ ) and root water uptake ( $\delta E_i$ ) based on the spatial deviation from  
 397 the mean during the defined dry periods. Soil moisture sensor locations colored according to throughfall input. Soil moisture  
 398 sensor locations are colored from lighter to darker in the throughout figure according to throughfall input.

### 399 **3.4) Fixed factors regulating root water uptake patterns**

400 We used a linear mixed effects model to disentangle the effects of throughfall, soil water, soil properties,  
 401 and the neighbouring tree characteristics on root water uptake patterns. The fixed and random effects  
 402 contributed almost equally to the model. The  $R^2$  of the model was 0.77, and the contribution of the fixed  
 403 effect to the  $R^2$  was 0.39 (See the supplement for more details on the optimal model).

404 Figure 4 shows only the significant fixed effects for root water uptake patterns. Spatial deviation of soil  
 405 water from the mean (i.e., soil water patterns) was the only single and the most significant factor positively

406 related to the spatial deviation of root water uptake. Thus, water uptake was elevated at locations where  
407 the most water was retained in the soil at the given time, i.e., greater soil water storage.



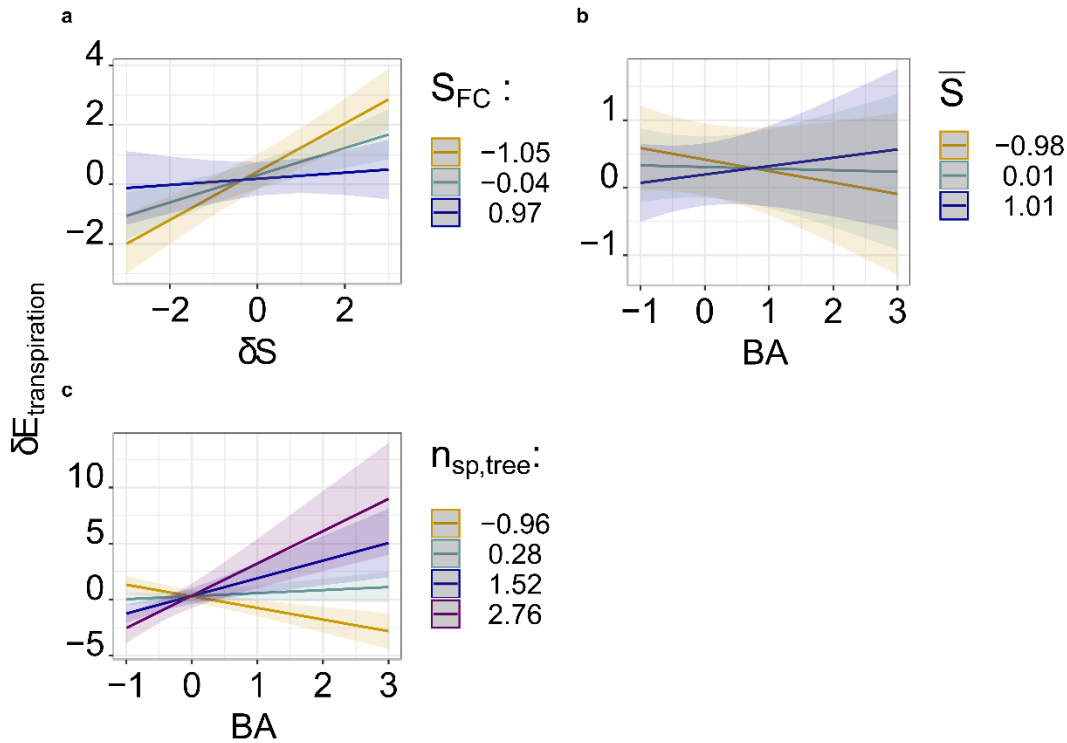
408

409 **Figure 4** The significant fixed factors of the best model to estimate root water uptake patterns ( $\delta E_i$ ). Values on the x-axis  
410 indicate the slope of the relations. All variables were scaled by Z-transformation. Interaction is shown with 'x'. Here  $\delta S$  is the  
411 spatial deviation of soil water,  $S_{FC}$  is the field capacity,  $n_{sp,tree}$  is the number of species, BA is the basal area, and  $\bar{S}$  is soil water  
412 storage. Significance codes are \*\*\*  $\cong 0$ , \*\*  $\cong 0.001$ . (the details on the model can be found in the supplement)

413 Field capacity by itself was not a significant factor affecting local root water uptake. However, it strongly  
414 influenced how local soil water controlled root water uptake as a part of the significant interaction term.  
415 Figure 5a illustrates how to root water uptake was more dependent on local soil water when field capacity  
416 was low (i.e., higher macroporosity). In contrast, soil bulk density and therefore total porosity was not  
417 part of the final model.

418 Although the spatial average of soil water storage, e.g., the state of wetness, was not an important factor  
419 for local root water uptake by itself, it moderated the impact of basal area (BA) on the spatial distribution  
420 of water uptake. We found that as the plot dries, uptake shifts from places with higher to places with lower  
421 basal area (Figure 5b). Furthermore, the statistical model revealed that water uptake increased with the  
422 higher basal area at locations where multiple species co-existed (Figure 5c). However, the number of  
423 species and the basal area were individually not significant fixed effects. Lastly, throughfall patterns were  
424 not significant predictors of local root water uptake. Only the median of the spatial deviation of

425 throughfall, which represents temporally stable patterns within the sampling period ( $\widehat{\delta P_{TF}}$ ), marginally  
426 improved the final model.



427

428 **Figure 5** Visualisation of the significant relations shown in Figure 4, representing the significant drivers of root water uptake  
429 patterns during the defined dry periods. Relation to (a) interactive relation of the spatial deviation of soil water storage and  
430 field capacity ( $S_{FC}$ ), (b) the interactive relation of basal area (BA) and the spatial average of soil water storage ( $\bar{S}$ ), (c) the  
431 interactive relation of number of species ( $n_{sp,tree}$ ) and basal area (BA.).

#### 432 **4) Discussion**

433 We investigated the role of throughfall, soil water patterns, and soil and tree characteristics on the spatial  
434 variation of root water uptake. In the following sections we discuss three main findings, which are: (1)  
435 Contrary to our hypothesis, throughfall patterns do not play a role not in root water uptake patterns despite  
436 the recurrence of distinctly localized greater and lesser throughfall inputs. (2) How and where water is  
437 stored in the soil, which is strongly determined by soil hydraulic properties, dominates water uptake  
438 patterns. (3) The size and species of neighbouring trees regulate relative local water uptake such that  
439 locations surrounded by more diverse neighbourhoods are subject to greater water uptake.

#### 440 **4.1) Spatial variation in throughfall does not affect root water uptake patterns**

441 We adequately captured the spatial distribution and temporal stability of throughfall at locations where  
442 local root water uptake was derived. Consistent with previous observations in temperate forests (e.g.,  
443 Whelan and Anderson, 1996; Staelens et al., 2006; Metzger et al., 2017), the amount of weekly rainfall  
444 significantly altered the spatial distribution of throughfall such that more rainfall, and thus more  
445 throughfall, resulted in less spatial variability. Previous studies repeatedly showed that throughfall  
446 patterns exhibit temporal stability in forest ecosystems (e.g., Keim et al., 2005; Staelens et al., 2006;  
447 Wullaert et al., 2009; Rodrigues et al., 2022). At our research site, using event-based sampling, Metzger  
448 et al., (2017) and Fischer-Bedtke et al., (2023) demonstrated that throughfall patterns persist over time,  
449 which was also true for our weekly sampling in 2019. With canopy cover being the key driver of  
450 throughfall (Fischer-Bedtke et al., 2023), it is not surprising that weekly cumulative events resulted in a  
451 localized high and low throughfall input.

452 Contrary to expectations (Bouten et al., 1992; Guswa and Spence, 2012; Coenders-Gerrits et al., 2013;  
453 Fischer-Bedtke et al., 2023), our results showed that throughfall hotspots do not increase or facilitate  
454 greater root water uptake. In addition, the linear mixed effects model results confirmed that throughfall  
455 patterns do not drive the variation in root water uptake. We attributed the absence of this to two reasons:  
456 (1) decoupled soil water and throughfall patterns, (2) non-water limited conditions.

457 Regarding (1), we confirmed that the temporally stable throughfall patterns do not correspond to the post-  
458 event soil water and root water uptake patterns. We paired the measurements of throughfall and soil water  
459 content measurements – and thus the estimates of root water uptake- within a distance of 1 m. The spatial  
460 correlation length of soil water content and throughfall is on the order of 6-10 m in natural temperate  
461 forests (Keim et al., 2005; Gerrits et al., 2010; Zehe et al., 2010). In the same study site with the spatially  
462 extended throughfall sampling, Fischer-Bedtke et al., (2023) found that the throughfall correlation length  
463 increased with decreasing event size, varying from 6.2 m to 9.5 m depending on the size of the rain events.  
464 Thus, the paired sampling design in our study likely provided co-located throughfall and soil moisture  
465 measurements. However, variation in soil water storage was not related to throughfall patterns despite  
466 temporally persistent local high and low throughfall inputs.

467 Some studies, mostly conducted in the arid regions and coniferous forests, reported that soil wetting  
468 patterns were not or only partly linked to throughfall variation, despite recurrent throughfall patterns (Raat  
469 et al., 2002; Shachnovich et al., 2008; Zhu et al., 2021). Forest floor thickness, horizontal water flow, and  
470 soil properties were suggested as reasons for the decoupled patterns. Other modelling and field studies  
471 conducted in temperate deciduous forests found that throughfall patterns influenced soil moisture  
472 response to rain event rather than post-event soil water storage variability (Coenders-Gerrits et al., 2013;  
473 Metzger et al., 2017; Fischer et al., 2023). These studies attributed possible reasons to local processes  
474 such as preferential flow due to soil water repellency, the soil pore structure, or elevated root water uptake.  
475 Our results support that it is not root water uptake but preferential flow paths that are likely to decouple  
476 the throughfall and soil water patterns. In fact, Fischer-Bedtke et al., (2023) using independent throughfall  
477 and soil water content sampling designs, demonstrated that the signature of throughfall patterns dissipated  
478 in the post-event soil water variation. However, they detected the stronger influence of throughfall  
479 patterns in the soil moisture response to rainfall in the 2015 and 2016 growing seasons. The temporal  
480 variation in soil water content in the 2019 growing season was similar to the seasonal decline in soil water  
481 content in 2015 (Metzger et al., 2017). Dry soil conditions can lead to rapid drainage due to reduced water  
482 holding capability (Jost et al., 2004; Blume et al., 2009; Wiekenkamp et al., 2016; Demand et al., 2019;  
483 Molina et al., 2019) regardless of throughfall amount and its variation. Therefore, our findings support  
484 that the localized throughfall input potentially enhances preferential flow because of low soil retention  
485 (Fischer-Bedtke et al., 2023) rather than local root water uptake. As a result, the fast flow processes likely  
486 dominate how water is stored and transported at our site, erasing the throughfall distribution signature in  
487 soil water and root water uptake patterns. Moreover, any short-term response of uptake to throughfall  
488 could not be captured as water uptake was calculated only after 56 hours had elapsed since the last rain  
489 event, yet we showed that temporally stable hotspots are not associated with elevated water uptake.  
490 Hence, our results are consistent with previous propositions stating that the spatial variation of throughfall  
491 affects drainage and subsurface flow (Keim et al., 2006; Blume et al., 2009; Guswa and Spence, 2012),  
492 while root activities such as water uptake and hydraulic redistribution do not alter canopy-attributed  
493 heterogeneity in drainage pathways (Guswa, 2012).



494 The second reason (2) is related to water-limitation conditions. In central Europe, 2019 was the second  
495 consecutive extremely dry summer (Boergens et al., 2020), which damaged beech forests (Obladen et al.,  
496 2021). On average, however, the potential evapotranspiration demand was met at the study site despite  
497 the low soil water storage. The ratio of root water uptake to potential evapotranspiration was mostly above  
498 65%, which is within the expected range even in the absence of shallow groundwater storage (Nie et al.,  
499 2021). Hence, local biotic and soil tied abiotic factors determined the spatial variation of root water uptake  
500 during growing season rather than throughfall -water input- patterns. However, the discrepancy between  
501 daily potential evapotranspiration and root water uptake only increased as the soil in the sampled layers  
502 dried out, due to a potential shift in the water uptake depth (see below).

#### 503 **4. 2) Relative and average soil wetness shapes root water uptake patterns**

504 We found that spatial variation in soil water storage strongly regulates local water uptake such that wetter  
505 locations enhance root water uptake. This finding is consistent with expectations as transpiration rate  
506 relies on soil water availability and distribution (Couvreur et al., 2014; Klein et al., 2014; Hildebrandt et  
507 al., 2016). Here, we provide further support that root water uptake is likely to reduce the spatial variability  
508 in soil water storage as has been previously suggested (Hopmans and Bristow, 2002; Ivanov et al., 2010;  
509 Neumann and Cardon, 2012).

510 Trees take up more water in locations where water is not subject to throughfall-driven rapid drainage (see  
511 above), as a result root water uptake patterns are determined by where water is retained longer in the soil.  
512 Our results support previous studies suggesting that tree transpiration demand is met by water with longer  
513 residence time in the soil matrix - passive storage - while groundwater recharge is fed by rapid flow -  
514 active storage (e.g, Evaristo et al., 2019; Sprenger et al., 2019). In our statistical analyses, we investigated  
515 the soil properties of bulk density and field capacity, which are strongly dependent on other soil properties  
516 that control aggregation and soil structure. Although bulk density is strongly related to texture, porosity,  
517 soil organic carbon content , , all of which also affect water retention (Zacharias and Wessolek, 2007;  
518 Looy et al., 2017), surprisingly soil bulk density was not retained as a predictive variable in the optimal  
519 model. In contrast, the interaction term including field capacity and local soil water storage was significant  
520 in the model with a negative relationship with relative water uptake, showing that the combination of

521 higher field capacity (fewer macropores) and low soil water hinders water uptake because water more is  
522 more strongly bound in the soil. Differences in local soil properties regulate the matric potential at a  
523 certain soil wetness. Thus, wetter locations do not necessarily correspond to those of easier root water  
524 uptake due to differences in the soil water retention characteristics (Vereecken et al., 2007; Cai et al.,  
525 2018) for which field capacity serves as a proxy. However soil properties alone were less important  
526 (smaller effects size of the interaction term including field capacity) than other factors despite their control  
527 on the spatial distribution of soil moisture (Vereecken et al., 2022).

528 In addition, the spatial mean of soil water - a measure of overall wetness of the stand - influenced root  
529 water uptake patterns, yet the effect depended on the basal area of neighboring trees. We found that as  
530 the study site dries out, local water uptake increased in locations with smaller basal areas. Conversely,  
531 wetter site conditions facilitate greater water uptake at locations with higher basal areas, i.e., dense  
532 clusters of large trees. We interpret this as a sign that larger trees are likely to shift their water uptake to  
533 deeper soil layers to meet transpiration demands, beyond the monitored soil depth (37 cm), as follows:  
534 Higher basal area is likely to increase transpiration demand and enhance water uptake as long as water is  
535 available. Moreover, locations with higher basal area exhaust the water storage more rapidly as these  
536 locations host larger root structure and root biomass (Le Goff and Ottorini, 2001). At the same time, larger  
537 sized trees can shift uptake to deeper layers (Gaines et al., 2016).

538 Beech trees have extensive root systems at shallower depths similar to other temperate tree species, such  
539 as European ash and sycamore maple (Kreuzwieser and Gessler, 2010; Brinkmann et al., 2019) Despite  
540 their shallower root system (Leuschner, 2020) in response to declining soil water content in the topsoil,  
541 temperate tree species can tap water from the deeper soil layers (Brinkmann et al., 2019; Agee et al.,  
542 2021; Seeger and Weiler, 2021). Recently, Agee et al. (2021) used a three-dimensional water uptake  
543 model based on observations in temperate mixed-deciduous forest to show that water uptake is shifted to  
544 the deeper soil layers as soil moisture depletes, which is consistent with the field observations. Moreover,  
545 Krämer and Hölscher (2010) observed in beech and mixed deciduous stands that roots can extract water  
546 at depths down to 70 cm soil depth. Similar to our site, theirs had a shallow soil layer underlain by  
547 weathered limestone, but the soil depth varied between 50 and 120 cm. Brinkmann et al., (2019) also

548 observed similar depth range for beech-trees in a mixed forest by tracing stable water isotopes of soil and  
549 xylem water.

550 Further tree age and size can affect both individual and stand level transpiration because of the different  
551 physiological characteristics and biometrics of trees associated with them (Kostner et al., 2002; Tsuruta  
552 et al., 2023). Within the same species, the larger -presumably older- trees have an advantage in accessing  
553 the deeper water storages because of their larger root biomass (Le Goff and Ottorini, 2001) and root  
554 plasticity may be able to shift the depth of water uptake while younger trees rely on shallower soil water  
555 storages (Dawson, 1996). Our results can be interpreted as tree size, which can be attributed to tree age,  
556 affecting root water uptake patterns through differential root biomass development. Furthermore, in the  
557 Hainich the coexisting species most likely represent highly coherent rooting depth distribution among  
558 trees (Gebauer et al., 2012; Meinen et al., 2009) yet adopt different water uptake strategies (see below).  
559 Hence consistent with previous studies focusing on temperate tree species, the linear mixed effect model  
560 results indicate that trees of different sizes response to declining soil water content by shifting water  
561 uptake depth.

### 562 **4.3) Tree species richness regulates root water uptake patterns**

563 In addition to the basal area, we included the number of species and number of tree individuals in the  
564 linear mixed effects analysis to further explore the biotic drivers of root water uptake patterns. While the  
565 number of trees was unimportant, the number of species and the basal area showed a significant  
566 interaction effect on the local water uptake. The result indicates that an increase in species richness leads  
567 to greater root water uptake, depending on the size and/or density of the neighboring trees: Higher basal  
568 area, combined with more species, elevates water uptake. In other words, the interactions among  
569 neighboring tree species strongly determine root water uptake patterns, and for the same basal area, more  
570 water can be taken up in a diverse neighborhood than in a less diverse locations.

571 In temperate forests, transpiration has been observed to change with tree species richness at the stand  
572 level (Krämer and Hölscher, 2010; Gebauer et al., 2012; Kunert et al., 2012; Meißner et al., 2012;  
573 Forrester, 2014). Although some studies indicate a positive relationship between tree diversity and water  
574 uptake rate (Forrester et al., 2010; Krämer and Hölscher, 2010; Kunert et al., 2012), tree species diversity

575 is not always positively related to water uptake. While Krämer and Hölscher (2010) observed a positive  
576 correlation between water uptake and species richness of the plots in the upper soil layers during soil  
577 drying in 2006 at the same study site, Meißner et al. (2012) found no relationship between tree diversity  
578 and root water uptake in 2009. They attributed this finding to wetter soil conditions. In contrast, Lübbe et  
579 al. (2016) observed a weak effect of diversity on transpiration in wetter soil conditions but not in drier  
580 conditions compared to previous studies (e.g., Pretzsch et al., 2013; del Río et al., 2014). Shortage of  
581 water can inflate competition mechanisms for water among tree species (González de Andrés et al., 2018;  
582 Vitali et al., 2018; Magh et al., 2020). Our results indicate that competition between neighboring tree  
583 species increases water uptake capacity at more diverse spots (Wambsganss et al., 2021).

584 In addition, different co-existing tree species can facilitate resource uptake or reduce competition,  
585 depending on the temporal and spatial availability of the sources, which is often defined as  
586 complementarity (Forrester and Bauhus, 2016). As reviewed and listed by Silvertown et al. (2015),  
587 several studies suggest that co-existing tree species reduce competition for subsurface water sources by  
588 adopting different vertical root water uptake strategies, referred to as hydrological niche partitioning. In  
589 addition, trees can transport water from wet to dry parts of the soil layers through their roots (Neumann  
590 and Cardon, 2012). The mechanism is called hydraulic redistribution or hydraulic lift, which can provide  
591 water availability to the shallow roots in drier layers (Burgess et al., 1998; Jonard et al., 2011; Hafner et  
592 al., 2017; Lee et al., 2018; Rodríguez-Robles et al., 2020; Hafner et al., 2021). In an experiment with six  
593 temperate tree species, including the European beech, Hafner et al. (2021) found that the neighboring tree  
594 species diversity may not be important for exploiting water uptake through hydraulic redistribution. Both  
595 hydraulic niche partitioning and redistribution have been observed vertically, whereas horizontal patterns  
596 are largely unexplored the context of niche partitioning (Hildebrandt, 2020). Our results do not provide  
597 direct evidence for either hydraulic redistribution or horizontal niche partitioning. However, they indicate  
598 that horizontal root water uptake patterns are regulated by species richness and interactions among  
599 neighbouring trees. Thus, we emphasize here the complex interplay between tree species diversity,  
600 complementary mechanisms, and water uptake patterns, which is consistent not only with the above-  
601 mentioned plot-scale studies, but also with larger-scale studies. For instance Knighton et al., (2019) using  
602 the Budyko framework across more than one hundred catchments found that transpiration losses in

603 catchments with deep rooted and mixed species forests differed from those in monoculture catchments.  
604 In other words, both plot and catchment scale studies support our results showing that interactions among  
605 different coexisting species play a significant role in the spatio-temporal variation of root water uptake.

## 606 **5) Conclusion**

607 We investigated the factors that influence the spatial patterns of root water uptake by considering  
608 heterogeneity in throughfall and soil water. To that end, we acquired a comprehensive data set based on  
609 throughfall measurements paired with soil moisture sensors in a mixed deciduous forest. Soil and  
610 neighboring tree characteristics were also included in the linear mixed effects model. We found that  
611 variation in root water uptake did not correspond to throughfall consequently rejecting our hypothesis  
612 that variation in throughfall is imprinted in water uptake patterns. Wetter soil locations, also poorly  
613 associated with higher throughfall, increased local root water uptake. In contrast, how average soil water  
614 conditions modified root water uptake depended on the neighborhood basal area. As the site dried out,  
615 large trees likely took up water in deeper layers to meet transpiration demands. Furthermore, an increase  
616 in species diversity promoted root water uptake, similarly depending on the size of neighboring trees,  
617 suggesting active complementarity mechanisms in the forest stand. In conclusion, our results manifest  
618 that soil water distribution and neighboring tree characteristics regulate root water uptake patterns more  
619 than soil properties and throughfall variation.

620

## 621 **Acknowledgments**

622 This study is part of the Collaborative Research Centre (CRC 1076 AquaDiva) of the Friedrich Schiller  
623 University Jena, funded by the Deutsche Forschungsgemeinschaft (DFG, German Research  
624 Foundation)—SFB 1076—Project Number 218627073. We thank to AquaDiva subproject D03 for  
625 weather station (Reckenbuel) data. Also, people who contributed to installation of soil moisture sensors  
626 in the research site: Ricardo Ontiveros-Enriques, Bernd Ruppe, Danny Schelhorn, Josef Weckmüller. We  
627 thank the Hainich CZE site manager Robert Lehmann and the Hainich National Park. We thank the

628 bachelor and master students Carla Peter, Xiaoyu Zhao, Stephan Bock for their contribution to throughfall  
629 sampling.

630

### 631 **Data availability**

632 The dataset is currently being prepared for publication in an official repository. The DOI will be published  
633 with the data at the latest when the data are published.

634

### 635 **Author contributions**

636 GD and AH designed the throughfall measurement setup, AH and JCM designed soil moisture  
637 measurement. GD conducted the field sampling with assistance from JF and the students listed in the  
638 Acknowledgments. GD analyzed the data, developed the linear mixed effects model, and analyzed the  
639 results with AH and AG. GD prepared the first version of the manuscript, and all authors contributed to  
640 discussions and the final version of the manuscript.

### 641 **Competing interests**

642 Anke Hildebrandt is part of the editorial board of HESS. The peer-review process was guided by an  
643 independent editor, and the authors have also no other competing interests to declare.

644

## 645 **6) References**

646 Agee, E., He, L., Bisht, G., Couvreur, V., Shahbaz, P., Meunier, F., Gough, C. M., Matheny, A. M.,  
647 Bohrer, G., and Ivanov, V.: Root lateral interactions drive water uptake patterns under water limitation,  
648 *Advances in Water Resources*, 151, 103896, <https://doi.org/10.1016/j.advwatres.2021.103896>, 2021.

649 Bachmair, S., Weiler, M., and Troch, P. A.: Intercomparing hillslope hydrological dynamics: Spatio-  
650 temporal variability and vegetation cover effects, *Water Resources Research*, 48,  
651 <https://doi.org/10.1029/2011WR011196>, 2012.

652 Baroni, G., Ortuani, B., Facchi, A., and Gandolfi, C.: The role of vegetation and soil properties on the  
653 spatio-temporal variability of the surface soil moisture in a maize-cropped field, *Journal of Hydrology*,  
654 489, 148–159, <https://doi.org/10.1016/j.jhydrol.2013.03.007>, 2013.

655 Bartoń, K.: MuMIn: Multi-Model Inference, 2020.

- 656 Bates, D., Mächler, M., Bolker, B., and Walker, S.: Fitting Linear Mixed-Effects Models Using **lme4**, J.  
657 Stat. Soft., 67, <https://doi.org/10.18637/jss.v067.i01>, 2015.
- 658 Blume, T., Zehe, E., and Bronstert, A.: Use of soil moisture dynamics and patterns at different spatio-  
659 temporal scales for the investigation of subsurface flow processes, *Hydrology and Earth System Sciences*,  
660 13, 1215–1233, <https://doi.org/10.5194/hess-13-1215-2009>, 2009.
- 661 Boergens, E., Güntner, A., Dobslaw, H., and Dahle, C.: Quantifying the Central European Droughts in  
662 2018 and 2019 With GRACE Follow-On, *Geophysical Research Letters*, 47, e2020GL087285,  
663 <https://doi.org/10.1029/2020GL087285>, 2020.
- 664 Bogena, H. R., Herbst, M., Huisman, J. A., Rosenbaum, U., Weuthen, A., and Vereecken, H.: Potential  
665 of Wireless Sensor Networks for Measuring Soil Water Content Variability, *Vadose Zone Journal*, 9,  
666 1002–1013, <https://doi.org/10.2136/vzj2009.0173>, 2010.
- 667 Borchers, H. W.: *pracma: Practical Numerical Math Functions*, 2021.
- 668 Bouten, W., Heimovaara, T. J., and Tiktak, A.: Spatial patterns of throughfall and soil water dynamics in  
669 a Douglas fir stand, *Water Resources Research*, 28, 3227–3233, <https://doi.org/10.1029/92WR01764>,  
670 1992.
- 671 Brinkmann, N., Eugster, W., Buchmann, N., and Kahmen, A.: Species-specific differences in water  
672 uptake depth of mature temperate trees vary with water availability in the soil, *Plant Biology*, 21, 71–81,  
673 <https://doi.org/10.1111/plb.12907>, 2019.
- 674 Brum, M., Vadeboncoeur, M. A., Ivanov, V., Asbjornsen, H., Saleska, S., Alves, L. F., Penha, D., Dias,  
675 J. D., Aragão, L. E. O. C., Barros, F., Bittencourt, P., Pereira, L., and Oliveira, R. S.: Hydrological niche  
676 segregation defines forest structure and drought tolerance strategies in a seasonal Amazon forest, *Journal*  
677 *of Ecology*, 107, 318–333, <https://doi.org/10.1111/1365-2745.13022>, 2019.
- 678 Burgess, S. S. O., Adams, M. A., Turner, N. C., and Ong, C. K.: The redistribution of soil water by tree  
679 root systems, *Oecologia*, 115, 306–311, <https://doi.org/10.1007/s004420050521>, 1998.
- 680 Cai, G., Vanderborght, J., Langensiepen, M., Schnepf, A., Hüging, H., and Vereecken, H.: Root growth,  
681 water uptake, and sap flow of winter wheat in response to different soil water conditions, *Hydrol. Earth*  
682 *Syst. Sci.*, 22, 2449–2470, <https://doi.org/10.5194/hess-22-2449-2018>, 2018.
- 683 Cardon, G. E. and Letey, J.: Plant Water Uptake Terms Evaluated for Soil Water and Solute Movement  
684 Models, *Soil Science Society of America Journal*, 56, 1876–1880,  
685 <https://doi.org/10.2136/sssaj1992.03615995005600060038x>, 1992.

- 686 Carlyle-Moses, Darryl. E., Lishman, Chad. E., and McKee, Adam. J.: A preliminary evaluation of  
687 throughfall sampling techniques in a mature coniferous forest, *Journal of Forestry Research*, 25, 407–  
688 413, <https://doi.org/10.1007/s11676-014-0468-8>, 2014.
- 689 Coenders-Gerrits, A. M. J., Hopp, L., Savenije, H. H. G., and Pfister, L.: The effect of spatial throughfall  
690 patterns on soil moisture patterns at the hillslope scale, *Hydrol. Earth Syst. Sci.*, 17, 1749–1763,  
691 <https://doi.org/10.5194/hess-17-1749-2013>, 2013.
- 692 Cosh, M. H., Jackson, T. J., Moran, S., and Bindlish, R.: Temporal persistence and stability of surface  
693 soil moisture in a semi-arid watershed, *Remote Sensing of Environment*, 112, 304–313,  
694 <https://doi.org/10.1016/j.rse.2007.07.001>, 2008.
- 695 Couvreur, V., Vanderborght, J., Beff, L., and Javaux, M.: Horizontal soil water potential heterogeneity:  
696 simplifying approaches for crop water dynamics models, *Hydrology and Earth System Sciences*, 18,  
697 1723–1743, <https://doi.org/10.5194/hess-18-1723-2014>, 2014.
- 698 Crockford, R. H. and Richardson, D. P.: Partitioning of rainfall into throughfall, stemflow and  
699 interception: effect of forest type, ground cover and climate, *Hydrological Processes*, 14, 2903–2920,  
700 2000.
- 701 Dawson, T. E.: Determining water use by trees and forests from isotopic, energy balance and transpiration  
702 analyses: the roles of tree size and hydraulic lift, *Tree Physiology*, 16, 263–272,  
703 <https://doi.org/10.1093/treephys/16.1-2.263>, 1996.
- 704 Demand, D., Blume, T., and Weiler, M.: Spatio-temporal relevance and controls of preferential flow at  
705 the landscape scale, *Hydrol. Earth Syst. Sci.*, 23, 4869–4889, <https://doi.org/10.5194/hess-23-4869-2019>,  
706 2019.
- 707 Demir, G., Michalzik, B., Filipzik, J., Metzger, J., and Hildebrandt, A.: Spatial variation of grassland  
708 canopy affects soil wetting patterns and preferential flow,  
709 <https://doi.org/10.22541/au.164970545.54927607/v1>, 2022.
- 710 Dunkerley, D.: Stemflow on the woody parts of plants: dependence on rainfall intensity and event profile  
711 from laboratory simulations, *Hydrological Processes*, 28, 5469–5482, <https://doi.org/10.1002/hyp.10050>,  
712 2014.
- 713 Emerman, S. H. and Dawson, T. E.: Hydraulic Lift and Its Influence on the Water Content of the  
714 Rhizosphere: An Example from Sugar Maple, *Acer saccharum*, *Oecologia*, 108, 273–278, 1996.
- 715 Evaristo, J., Kim, M., van Haren, J., Pangle, L. A., Harman, C. J., Troch, P. A., and McDonnell, J. J.:  
716 Characterizing the Fluxes and Age Distribution of Soil Water, Plant Water, and Deep Percolation in a  
717 Model Tropical Ecosystem, *Water Resources Research*, 55, 3307–3327,  
718 <https://doi.org/10.1029/2018WR023265>, 2019.



- 719 Fan, J., Oestergaard, K. T., Guyot, A., Jensen, D. G., and Lockington, D. A.: Spatial variability of  
720 throughfall and stemflow in an exotic pine plantation of subtropical coastal Australia, *Hydrological*  
721 *Processes*, 29, 793–804, <https://doi.org/10.1002/hyp.10193>, 2015.
- 722 Fischer, C., Metzger, J. C., Demir, G., Wutzler, T., and Hildebrandt, A.: Throughfall spatial patterns  
723 translate into spatial patterns of soil moisture dynamics – empirical evidence, *Ecohydrology/Instruments*  
724 *and observation techniques*, <https://doi.org/10.5194/hess-2022-418>, 2023.
- 725 Fischer-Bedtke, C., Metzger, J. C., Demir, G., Wutzler, T., and Hildebrandt, A.: Throughfall spatial  
726 patterns translate into spatial patterns of soil moisture dynamics – empirical evidence, *Hydrology and*  
727 *Earth System Sciences*, 27, 2899–2918, <https://doi.org/10.5194/hess-27-2899-2023>, 2023.
- 728 Forrester, D. I.: The spatial and temporal dynamics of species interactions in mixed-species forests: From  
729 pattern to process, *Forest Ecology and Management*, 312, 282–292,  
730 <https://doi.org/10.1016/j.foreco.2013.10.003>, 2014.
- 731 Forrester, D. I. and Bauhus, J.: A Review of Processes Behind Diversity—Productivity Relationships in  
732 Forests, *Curr Forestry Rep*, 2, 45–61, <https://doi.org/10.1007/s40725-016-0031-2>, 2016.
- 733 Forrester, D. I., Theiveyanathan, S., Collopy, J. J., and Marcar, N. E.: Enhanced water use efficiency in a  
734 mixed Eucalyptus globulus and Acacia mearnsii plantation, *Forest Ecology and Management*, 259, 1761–  
735 1770, <https://doi.org/10.1016/j.foreco.2009.07.036>, 2010.
- 736 Gaines, K. P., Stanley, J. W., Meinzer, F. C., McCulloh, K. A., Woodruff, D. R., Chen, W., Adams, T.  
737 S., Lin, H., and Eissenstat, D. M.: Reliance on shallow soil water in a mixed-hardwood forest in central  
738 Pennsylvania, *Tree Physiol*, 36, 444–458, <https://doi.org/10.1093/treephys/tpv113>, 2016.
- 739 Gebauer, T., Horna, V., and Leuschner, C.: Canopy transpiration of pure and mixed forest stands with  
740 variable abundance of European beech, *Journal of Hydrology*, 442–443, 2–14,  
741 <https://doi.org/10.1016/j.jhydrol.2012.03.009>, 2012.
- 742 Gerrits, A. M. J., Pfister, L., and Savenije, H. H. G.: Spatial and temporal variability of canopy and forest  
743 floor interception in a beech forest, *Hydrol. Process.*, 24, 3011–3025, <https://doi.org/10.1002/hyp.7712>,  
744 2010.
- 745 González de Andrés, E., Camarero, J. J., Blanco, J. A., Imbert, J. B., Lo, Y.-H., Sangüesa-Barreda, G.,  
746 and Castillo, F. J.: Tree-to-tree competition in mixed European beech–Scots pine forests has different  
747 impacts on growth and water-use efficiency depending on site conditions, *Journal of Ecology*, 106, 59–  
748 75, <https://doi.org/10.1111/1365-2745.12813>, 2018.
- 749 Grayson, R. B., Western, A. W., Chiew, F. H. S., and Blöschl, G.: Preferred states in spatial soil moisture  
750 patterns: Local and nonlocal controls, *Water Resources Research*, 33, 2897–2908,  
751 <https://doi.org/10.1029/97WR02174>, 1997.

- 752 Guderle, M. and Hildebrandt, A.: Using measured soil water contents to estimate evapotranspiration and  
753 root water uptake profiles – a comparative study, *Hydrol. Earth Syst. Sci.*, 17, 2015.
- 754 Guderle, M., Bachmann, D., Milcu, A., Gockele, A., Bechmann, M., Fischer, C., Roscher, C., Landais,  
755 D., Ravel, O., Devidal, S., Roy, J., Gessler, A., Buchmann, N., Weigelt, A., and Hildebrandt, A.: Dynamic  
756 niche partitioning in root water uptake facilitates efficient water use in more diverse grassland plant  
757 communities, *Funct Ecol*, 32, 214–227, <https://doi.org/10.1111/1365-2435.12948>, 2018.
- 758 Guo, J. S., Hungate, B. A., Kolb, T. E., and Koch, G. W.: Water source niche overlap increases with site  
759 moisture availability in woody perennials, *Plant Ecol*, 219, 719–735, [https://doi.org/10.1007/s11258-018-](https://doi.org/10.1007/s11258-018-0829-z)  
760 0829-z, 2018.
- 761 Guswa, A. J.: Canopy vs. Roots: Production and Destruction of Variability in Soil Moisture and  
762 Hydrologic Fluxes, *Vadose Zone Journal*, 11, vzj2011.0159, <https://doi.org/10.2136/vzj2011.0159>, 2012.
- 763 Guswa, A. J. and Spence, C. M.: Effect of throughfall variability on recharge: application to hemlock and  
764 deciduous forests in western Massachusetts, *Ecohydrology*, 5, 563–574, <https://doi.org/10.1002/eco.281>,  
765 2012.
- 766 Hafner, B. D., Tomasella, M., Häberle, K.-H., Goebel, M., Matyssek, R., and Grams, T. E. E.: Hydraulic  
767 redistribution under moderate drought among English oak, European beech and Norway spruce  
768 determined by deuterium isotope labeling in a split-root experiment, *Tree Physiology*, 37, 950–960,  
769 <https://doi.org/10.1093/treephys/tpx050>, 2017.
- 770 Hafner, B. D., Hesse, B. D., and Grams, T. E. E.: Friendly neighbours: Hydraulic redistribution accounts  
771 for one quarter of water used by neighbouring drought stressed tree saplings, *Plant, Cell & Environment*,  
772 44, 1243–1256, <https://doi.org/10.1111/pce.13852>, 2021.
- 773 Hildebrandt, A.: Root-Water Relations and Interactions in Mixed Forest Settings, in: *Forest-Water*  
774 *Interactions*, edited by: Levia, D. F., Carlyle-Moses, D. E., Iida, S., Michalzik, B., Nanko, K., and Tischer,  
775 A., Springer International Publishing, Cham, 319–348, [https://doi.org/10.1007/978-3-030-26086-6\\_14](https://doi.org/10.1007/978-3-030-26086-6_14),  
776 2020.
- 777 Hildebrandt, A., Kleidon, A., and Bechmann, M.: A thermodynamic formulation of root water uptake,  
778 *Hydrol. Earth Syst. Sci.*, 14, 2016.
- 779 Hopmans, J. W. and Bristow, K. L.: Current Capabilities and Future Needs of Root Water and Nutrient  
780 Uptake Modeling, in: *Advances in Agronomy*, vol. 77, Elsevier, 103–183, [https://doi.org/10.1016/S0065-](https://doi.org/10.1016/S0065-2113(02)77014-4)  
781 2113(02)77014-4, 2002.
- 782 Hupet, F. and Vanclooster, M.: Micro-variability of hydrological processes at the maize row scale:  
783 implications for soil water content measurements and evapotranspiration estimates, *Journal of Hydrology*,  
784 303, 247–270, <https://doi.org/10.1016/j.jhydrol.2004.07.017>, 2005.

- 785 Hupet, F., Lambot, S., Javaux, M., and Vanclooster, M.: On the identification of macroscopic root water  
786 uptake parameters from soil water content observations, *Water Resources Research*, 38, 36-1-36-14,  
787 <https://doi.org/10.1029/2002WR001556>, 2002.
- 788 IUSS Working Group, W. and others: World reference base for soil resources, *World Soil Resources*  
789 *Report*, 103, 2006.
- 790 Ivanov, V. Y., Fatichi, S., Jenerette, G. D., Espeleta, J. F., Troch, P. A., and Huxman, T. E.: Hysteresis  
791 of soil moisture spatial heterogeneity and the “homogenizing” effect of vegetation, *Water Resources*  
792 *Research*, 46, <https://doi.org/10.1029/2009WR008611>, 2010.
- 793 Jackisch, C., Knoblauch, S., Blume, T., Zehe, E., and Hassler, S. K.: Estimates of tree root water uptake  
794 from soil moisture profile dynamics, *Biogeosciences*, 17, 5787–5808, <https://doi.org/10.5194/bg-17-5787-2020>, 2020.
- 796 Jarecke, K. M., Bladon, K. D., and Wondzell, S. M.: The Influence of Local and Nonlocal Factors on Soil  
797 Water Content in a Steep Forested Catchment, *Water Resources Research*, 57, e2020WR028343,  
798 <https://doi.org/10.1029/2020WR028343>, 2021.
- 799 Jonard, F., André, F., Ponette, Q., Vincke, C., and Jonard, M.: Sap flux density and stomatal conductance  
800 of European beech and common oak trees in pure and mixed stands during the summer drought of 2003,  
801 *Journal of Hydrology*, 409, 371–381, <https://doi.org/10.1016/j.jhydrol.2011.08.032>, 2011.
- 802 Jost, G., Schume, H., and Hager, H.: Factors controlling soil water-recharge in a mixed European beech  
803 (*Fagus sylvatica* L.)–Norway spruce [*Picea abies* (L.) Karst.] stand, *Eur J Forest Res*, 123, 93–104,  
804 <https://doi.org/10.1007/s10342-004-0033-7>, 2004.
- 805 Katul, G. G. and Siqueira, M. B.: Biotic and abiotic factors act in coordination to amplify hydraulic  
806 redistribution and lift, *The New Phytologist*, 187, 3–6, 2010.
- 807 Keim, R. F., Skaugset, A. E., and Weiler, M.: Temporal persistence of spatial patterns in throughfall,  
808 *Journal of Hydrology*, 314, 263–274, <https://doi.org/10.1016/j.jhydrol.2005.03.021>, 2005.
- 809 Keim, R. F., Skaugset, A. E., and Weiler, M.: Storage of water on vegetation under simulated rainfall of  
810 varying intensity, *Advances in Water Resources*, 29, 974–986,  
811 <https://doi.org/10.1016/j.advwatres.2005.07.017>, 2006.
- 812 Kirchen, G., Calvaruso, C., Granier, A., Redon, P.-O., Van der Heijden, G., Bréda, N., and Turpault, M.-  
813 P.: Local soil type variability controls the water budget and stand productivity in a beech forest, *Forest*  
814 *Ecology and Management*, 390, 89–103, <https://doi.org/10.1016/j.foreco.2016.12.024>, 2017.

- 815 Kleidon, A. and Renner, M.: Thermodynamic limits of hydrologic cycling within the Earth system:  
816 concepts, estimates and implications, *Hydrol. Earth Syst. Sci.*, 17, 2873–2892,  
817 <https://doi.org/10.5194/hess-17-2873-2013>, 2013.
- 818 Kleidon, A., Renner, M., and Porada, P.: Estimates of the climatological land surface energy and water  
819 balance derived from maximum convective power, *Hydrol. Earth Syst. Sci.*, 18, 2201–2218,  
820 <https://doi.org/10.5194/hess-18-2201-2014>, 2014.
- 821 Klein, T., Rotenberg, E., Cohen-Hilaleh, E., Raz-Yaseef, N., Tatarinov, F., Preisler, Y., Ogée, J., Cohen,  
822 S., and Yakir, D.: Quantifying transpirable soil water and its relations to tree water use dynamics in a  
823 water-limited pine forest, *Ecohydrology*, 7, 409–419, <https://doi.org/10.1002/eco.1360>, 2014.
- 824 Knighton, J., Singh, K., and Evaristo, J.: Understanding Catchment-Scale Forest Root Water Uptake  
825 Strategies Across the Continental United States Through Inverse Ecohydrological Modeling, *Geophysical*  
826 *Research Letters*, 47, e2019GL085937, <https://doi.org/10.1029/2019GL085937>, 2019.
- 827 Kohlhepp, B., Lehmann, R., Seeber, P., Küsel, K., Trumbore, S. E., and Totsche, K. U.: Aquifer  
828 configuration and geostructural links control the groundwater quality in thin-bedded carbonate–  
829 siliciclastic alternations of the Hainich CZE, central Germany, *Hydrol. Earth Syst. Sci.*, 21, 6091–6116,  
830 <https://doi.org/10.5194/hess-21-6091-2017>, 2017.
- 831 Kostner, B., Falge, E., and Tenhunen, J. D.: Age-related effects on leaf area/sapwood area relationships,  
832 canopy transpiration and carbon gain of Norway spruce stands (*Picea abies*) in the Fichtelgebirge,  
833 Germany, *Tree Physiology*, 22, 567–574, <https://doi.org/10.1093/treephys/22.8.567>, 2002.
- 834 Krämer, I. and Hölscher, D.: Soil water dynamics along a tree diversity gradient in a deciduous forest in  
835 Central Germany, *Ecohydrology*, 3, 262–271, <https://doi.org/10.1002/eco.103>, 2010.
- 836 Kreuzwieser, J. and Gessler, A.: Global climate change and tree nutrition: influence of water availability,  
837 *Tree Physiology*, 30, 1221–1234, <https://doi.org/10.1093/treephys/tpq055>, 2010.
- 838 Kühnhammer, K., Kübert, A., Brüggemann, N., Deseano Diaz, P., van Dusschoten, D., Javaux, M., Merz,  
839 S., Vereecken, H., Dubbert, M., and Rothfuss, Y.: Investigating the root plasticity response of *Centaurea*  
840 *jacea* to soil water availability changes from isotopic analysis, *New Phytologist*, 226, 98–110,  
841 <https://doi.org/10.1111/nph.16352>, 2020.
- 842 Kunert, N., Schwendenmann, L., Potvin, C., and Hölscher, D.: Tree diversity enhances tree transpiration  
843 in a Panamanian forest plantation, *Journal of Applied Ecology*, 49, 135–144,  
844 <https://doi.org/10.1111/j.1365-2664.2011.02065.x>, 2012.
- 845 Küsel, K., Totsche, K. U., Trumbore, S. E., Lehmann, R., Steinhäuser, C., and Herrmann, M.: How Deep  
846 Can Surface Signals Be Traced in the Critical Zone? Merging Biodiversity with Biogeochemistry

- 847 Research in a Central German Muschelkalk Landscape, *Frontiers in Earth Science*, 4,  
848 <https://doi.org/10.3389/feart.2016.00032>, 2016.
- 849 Le Goff, N. and Ottorini, J.-M.: Root biomass and biomass increment in a beech (*Fagus sylvatica* L.)  
850 stand in North-East France, *Ann. For. Sci.*, 58, 1–13, <https://doi.org/10.1051/forest:2001104>, 2001.
- 851 Lee, E., Kumar, P., Barron-Gafford, G. A., Hendryx, S. M., Sanchez-Cañete, E. P., Minor, R. L., Colella,  
852 T., and Scott, R. L.: Impact of Hydraulic Redistribution on Multispecies Vegetation Water Use in a  
853 Semiarid Savanna Ecosystem: An Experimental and Modeling Synthesis, *Water Resour. Res.*, 54, 4009–  
854 4027, <https://doi.org/10.1029/2017WR021006>, 2018.
- 855 Leuschner, C.: Drought response of European beech (*Fagus sylvatica* L.)—A review, *Perspectives in*  
856 *Plant Ecology, Evolution and Systematics*, 47, 125576, <https://doi.org/10.1016/j.ppees.2020.125576>,  
857 2020.
- 858 Levia, D. F. and Frost, E. E.: A review and evaluation of stemflow literature in the hydrologic and  
859 biogeochemical cycles of forested and agricultural ecosystems, *Journal of Hydrology*, 274, 1–29,  
860 [https://doi.org/10.1016/S0022-1694\(02\)00399-2](https://doi.org/10.1016/S0022-1694(02)00399-2), 2003.
- 861 Levia, D. F. and Frost, E. E.: Variability of throughfall volume and solute inputs in wooded ecosystems,  
862 *Progress in Physical Geography: Earth and Environment*, 30, 605–632,  
863 <https://doi.org/10.1177/0309133306071145>, 2006.
- 864 Levia, D. F., Keim, R. F., Carlyle-Moses, D. E., and Frost, E. E.: Throughfall and Stemflow in Wooded  
865 Ecosystems, in: *Forest Hydrology and Biogeochemistry: Synthesis of Past Research and Future*  
866 *Directions*, edited by: Levia, D. F., Carlyle-Moses, D., and Tanaka, T., Springer Netherlands, Dordrecht,  
867 425–443, [https://doi.org/10.1007/978-94-007-1363-5\\_21](https://doi.org/10.1007/978-94-007-1363-5_21), 2011.
- 868 Levia, D. F., Hudson, S. A., Llorens, P., and Nanko, K.: Throughfall drop size distributions: a review and  
869 prospectus for future research: Throughfall drop size distributions, *WIREs Water*, 4, e1225,  
870 <https://doi.org/10.1002/wat2.1225>, 2017.
- 871 Lhomme, J.-P.: Formulation of root water uptake in a multi-layer soil-plant model: does van den Honert's  
872 equation hold?, *Hydrology and Earth System Sciences*, 2, 31–39, <https://doi.org/10.5194/hess-2-31-1998>,  
873 1998.
- 874 Looy, K. V., Bouma, J., Herbst, M., Koestel, J., Minasny, B., Mishra, U., Montzka, C., Nemes, A.,  
875 Pachepsky, Y. A., Padarian, J., Schaap, M. G., Tóth, B., Verhoef, A., Vanderborght, J., Ploeg, M. J. van  
876 der, Weihermüller, L., Zacharias, S., Zhang, Y., and Vereecken, H.: Pedotransfer Functions in Earth  
877 System Science: Challenges and Perspectives, *Reviews of Geophysics*, 55, 1199–1256,  
878 <https://doi.org/10.1002/2017RG000581>, 2017.

- 879 Lübke, T., Schuldt, B., Coners, H., and Leuschner, C.: Species diversity and identity effects on the water  
880 consumption of tree sapling assemblages under ample and limited water supply, *Oikos*, 125, 86–97,  
881 <https://doi.org/10.1111/oik.02367>, 2016.
- 882 Lüdecke, D., Ben-Shachar, M., Patil, I., Waggoner, P., and Makowski, D.: performance: An R Package  
883 for Assessment, Comparison and Testing of Statistical Models, *JOSS*, 6, 3139,  
884 <https://doi.org/10.21105/joss.03139>, 2021.
- 885 Magh, R.-K., Eiferle, C., Burzlaff, T., Dannenmann, M., Rennenberg, H., and Dubbert, M.: Competition  
886 for water rather than facilitation in mixed beech-fir forests after drying-wetting cycle, *Journal of*  
887 *Hydrology*, 587, 124944, <https://doi.org/10.1016/j.jhydrol.2020.124944>, 2020.
- 888 Magliano, P. N., Whitworth-Hulse, J. I., Florio, E. L., Aguirre, E. C., and Blanco, L. J.: Interception loss,  
889 throughfall and stemflow by *Larrea divaricata*: The role of rainfall characteristics and plant morphological  
890 attributes, *Ecological Research*, 34, 753–764, <https://doi.org/10.1111/1440-1703.12036>, 2019.
- 891 Martínez García, G., Pachepsky, Y. A., and Vereecken, H.: Effect of soil hydraulic properties on the  
892 relationship between the spatial mean and variability of soil moisture, *Journal of Hydrology*, 516, 154–  
893 160, <https://doi.org/10.1016/j.jhydrol.2014.01.069>, 2014.
- 894 Meinen, C., Leuschner, C., Ryan, N. T., and Hertel, D.: No evidence of spatial root system segregation  
895 and elevated fine root biomass in multi-species temperate broad-leaved forests, *Trees*, 23, 941–950,  
896 <https://doi.org/10.1007/s00468-009-0336-x>, 2009.
- 897 Meißner, M., Köhler, M., Schwendenmann, L., and Hölscher, D.: Partitioning of soil water among canopy  
898 trees during a soil desiccation period in a temperate mixed forest, *Biogeosciences*, 9, 3465–3474,  
899 <https://doi.org/10.5194/bg-9-3465-2012>, 2012.
- 900 Metzger, J. C., Wutzler, T., Valle, N. D., Filipzik, J., Grauer, C., Lehmann, R., Roggenbuck, M.,  
901 Schelhorn, D., Weckmüller, J., Küsel, K., Totsche, K. U., Trumbore, S., and Hildebrandt, A.: Vegetation  
902 impacts soil water content patterns by shaping canopy water fluxes and soil properties, *Hydrological*  
903 *Processes*, 31, 3783–3795, <https://doi.org/10.1002/hyp.11274>, 2017.
- 904 Metzger, J. C., Filipzik, J., Michalzik, B., and Hildebrandt, A.: Stemflow Infiltration Hotspots Create Soil  
905 Microsites Near Tree Stems in an Unmanaged Mixed Beech Forest, *Front. For. Glob. Change*, 4, 701293,  
906 <https://doi.org/10.3389/ffgc.2021.701293>, 2021.
- 907 Molina, A. J., Llorens, P., Garcia-Estringana, P., Moreno de las Heras, M., Cayuela, C., Gallart, F., and  
908 Latron, J.: Contributions of throughfall, forest and soil characteristics to near-surface soil water-content  
909 variability at the plot scale in a mountainous Mediterranean area, *Science of The Total Environment*, 647,  
910 1421–1432, <https://doi.org/10.1016/j.scitotenv.2018.08.020>, 2019.

- 911 Nadezhdina, N., Cermak, J., Meiresonne, L., and Ceulemans, R.: Transpiration of Scots pine in Flanders  
912 growing on soil with irregular substratum, *Forest Ecology and Management*, 9, 2007.
- 913 Neumann, R. B. and Cardon, Z. G.: The magnitude of hydraulic redistribution by plant roots: a review  
914 and synthesis of empirical and modeling studies, *New Phytologist*, 194, 337–352,  
915 <https://doi.org/10.1111/j.1469-8137.2012.04088.x>, 2012.
- 916 Nie, C., Huang, Y., Zhang, S., Yang, Y., Zhou, S., Lin, C., and Wang, G.: Effects of soil water content  
917 on forest ecosystem water use efficiency through changes in transpiration/evapotranspiration ratio,  
918 *Agricultural and Forest Meteorology*, 308–309, 108605,  
919 <https://doi.org/10.1016/j.agrformet.2021.108605>, 2021.
- 920 Obladen, N., Dechering, P., Skiadaresis, G., Tegel, W., Keßler, J., Höllerl, S., Kaps, S., Hertel, M.,  
921 Dulamsuren, C., Seifert, T., Hirsch, M., and Seim, A.: Tree mortality of European beech and Norway  
922 spruce induced by 2018-2019 hot droughts in central Germany, *Agricultural and Forest Meteorology*,  
923 307, 108482, <https://doi.org/10.1016/j.agrformet.2021.108482>, 2021.
- 924 Otto, J., Berveiller, D., Bréon, F.-M., Delpierre, N., Geppert, G., Granier, A., Jans, W., Knohl, A., Kuusk,  
925 A., Longdoz, B., Moors, E., Mund, M., Pinty, B., Schelhaas, M.-J., and Luysaert, S.: Forest summer  
926 albedo is sensitive to species and thinning: how should we account for this in Earth system models?,  
927 *Biogeosciences*, 11, 2411–2427, <https://doi.org/10.5194/bg-11-2411-2014>, 2014.
- 928 Pearson, R. K.: Data cleaning for dynamic modeling and control, in: 1999 European Control Conference  
929 (ECC), 1999 European Control Conference (ECC), 2584–2589,  
930 <https://doi.org/10.23919/ECC.1999.7099714>, 1999.
- 931 Pretzsch, H., Schütze, G., and Uhl, E.: Resistance of European tree species to drought stress in mixed  
932 versus pure forests: evidence of stress release by inter-specific facilitation, *Plant Biology*, 15, 483–495,  
933 <https://doi.org/10.1111/j.1438-8677.2012.00670.x>, 2013.
- 934 Priyadarshini, K. V. R., Prins, H. H. T., de Bie, S., Heitkönig, I. M. A., Woodborne, S., Gort, G., Kirkman,  
935 K., Ludwig, F., Dawson, T. E., and de Kroon, H.: Seasonality of hydraulic redistribution by trees to  
936 grasses and changes in their water-source use that change tree-grass interactions: HYDRAULIC  
937 REDISTRIBUTION BY TREES TO GRASSES AND CHANGES IN THEIR WATER SOURCES,  
938 *Ecohydrology*, 9, 218–228, <https://doi.org/10.1002/eco.1624>, 2016.
- 939 Pypker, T. G., Levia, D. F., Staelens, J., and Van Stan, J. T.: Canopy Structure in Relation to Hydrological  
940 and Biogeochemical Fluxes, in: *Forest Hydrology and Biogeochemistry: Synthesis of Past Research and  
941 Future Directions*, edited by: Levia, D. F., Carlyle-Moses, D., and Tanaka, T., Springer Netherlands,  
942 Dordrecht, 371–388, [https://doi.org/10.1007/978-94-007-1363-5\\_18](https://doi.org/10.1007/978-94-007-1363-5_18), 2011.
- 943 R Core Team: R: The R Project for Statistical Computing, R Foundation for Statistical Computing,  
944 Vienna, Austria, 2021.

- 945 Raat, K. J., Draaijers, G. P. J., Schaap, M. G., Tietema, A., and Verstraten, J. M.: Spatial variability of  
946 throughfall water and chemistry and forest floor water content in a Douglas fir forest stand, *Hydrol. Earth  
947 Syst. Sci.*, 6, 363–374, <https://doi.org/10.5194/hess-6-363-2002>, 2002.
- 948 del Río, M., Schütze, G., and Pretzsch, H.: Temporal variation of competition and facilitation in mixed  
949 species forests in Central Europe, *Plant Biology*, 16, 166–176, <https://doi.org/10.1111/plb.12029>, 2014.
- 950 Rodrigues, A. F., Terra, M. C. N. S., Mantovani, V. A., Cordeiro, N. G., Ribeiro, J. P. C., Guo, L., Nehren,  
951 U., Mello, J. M., and Mello, C. R.: Throughfall spatial variability in a neotropical forest: Have we  
952 correctly accounted for time stability?, *Journal of Hydrology*, 608, 127632,  
953 <https://doi.org/10.1016/j.jhydrol.2022.127632>, 2022.
- 954 Rodríguez-Robles, U., Arredondo, J. T., Huber-Sannwald, E., Yépez, E. A., and Ramos-Leal, J. A.:  
955 Coupled plant traits adapted to wetting/drying cycles of substrates co-define niche multidimensionality,  
956 *Plant, Cell & Environment*, 43, 2394–2408, <https://doi.org/10.1111/pce.13837>, 2020.
- 957 Rosenbaum, U., Bogena, H. R., Herbst, M., Huisman, J. A., Peterson, T. J., Weuthen, A., Western, A.  
958 W., and Vereecken, H.: Seasonal and event dynamics of spatial soil moisture patterns at the small  
959 catchment scale: DYNAMICS OF CATCHMENT-SCALE SOIL MOISTURE PATTERNS, *Water  
960 Resour. Res.*, 48, <https://doi.org/10.1029/2011WR011518>, 2012.
- 961 Rothfuss, Y. and Javaux, M.: Reviews and syntheses: Isotopic approaches to quantify root water uptake:  
962 a review and comparison of methods, *Biogeosciences*, 14, 2199–2224, <https://doi.org/10.5194/bg-14-2199-2017>, 2017.
- 964 Sadeghi, S. M. M., Gordon, D. A., and Van Stan II, J. T.: A Global Synthesis of Throughfall and Stemflow  
965 Hydrometeorology, in: *Precipitation Partitioning by Vegetation: A Global Synthesis*, edited by: Van Stan,  
966 I., John T., Gutmann, E., and Friesen, J., Springer International Publishing, Cham, 49–70,  
967 [https://doi.org/10.1007/978-3-030-29702-2\\_4](https://doi.org/10.1007/978-3-030-29702-2_4), 2020.
- 968 Schume, H., Jost, G., and Hager, H.: Soil water depletion and recharge patterns in mixed and pure forest  
969 stands of European beech and Norway spruce, *Journal of Hydrology*, 289, 258–274,  
970 <https://doi.org/10.1016/j.jhydrol.2003.11.036>, 2004.
- 971 Schwärzel, K., Menzer, A., Clausnitzer, F., Spank, U., Häntzschel, J., Grünwald, T., Köstner, B.,  
972 Bernhofer, C., and Feger, K.-H.: Soil water content measurements deliver reliable estimates of water  
973 fluxes: A comparative study in a beech and a spruce stand in the Tharandt forest (Saxony, Germany),  
974 *Agricultural and Forest Meteorology*, 149, 1994–2006, <https://doi.org/10.1016/j.agrformet.2009.07.006>,  
975 2009.
- 976 Seeger, S. and Weiler, M.: Temporal dynamics of tree xylem water isotopes: in situ monitoring and  
977 modeling, *Biogeosciences*, 18, 4603–4627, <https://doi.org/10.5194/bg-18-4603-2021>, 2021.



- 978 Shachnovich, Y., Berliner, P. R., and Bar, P.: Rainfall interception and spatial distribution of throughfall  
979 in a pine forest planted in an arid zone, *Journal of Hydrology*, 349, 168–177,  
980 <https://doi.org/10.1016/j.jhydrol.2007.10.051>, 2008.
- 981 Shani, U. and Dudley, L. M.: Modeling water uptake by roots under water and salt stress: Soil-based and  
982 crop response root sink terms, *Plant Roots: The Hidden Half*, 635–641, 1996.
- 983 Silvertown, J., Araya, Y., and Gowing, D.: Hydrological niches in terrestrial plant communities: a review,  
984 *Journal of Ecology*, 103, 93–108, <https://doi.org/10.1111/1365-2745.12332>, 2015.
- 985 Spanner, G. C., Gimenez, B. O., Wright, C. L., Menezes, V. S., Newman, B. D., Collins, A. D., Jardine,  
986 K. J., Negrón-Juárez, R. I., Lima, A. J. N., Rodrigues, J. R., Chambers, J. Q., Higuchi, N., and Warren, J.  
987 M.: Dry Season Transpiration and Soil Water Dynamics in the Central Amazon, *Frontiers in Plant  
988 Science*, 13, 2022.
- 989 Sprenger, M., Llorens, P., Cayuela, C., Gallart, F., and Latron, J.: Mechanisms of consistently disjunct  
990 soil water pools over (pore) space and time, *Hydrol. Earth Syst. Sci.*, 23, 2751–2762,  
991 <https://doi.org/10.5194/hess-23-2751-2019>, 2019.
- 992 Staelens, J., De Schrijver, A., Verheyen, K., and Verhoest, N. E. C.: Spatial variability and temporal  
993 stability of throughfall water under a dominant beech (*Fagus sylvatica* L.) tree in relationship to canopy  
994 cover, *Journal of Hydrology*, 330, 651–662, <https://doi.org/10.1016/j.jhydrol.2006.04.032>, 2006.
- 995 Staelens, J., De Schrijver, A., Verheyen, K., and Verhoest, N. E. C.: Rainfall partitioning into throughfall,  
996 stemflow, and interception within a single beech (*Fagus sylvatica* L.) canopy: influence of foliation, rain  
997 event characteristics, and meteorology, *Hydrological Processes*, 22, 33–45,  
998 <https://doi.org/10.1002/hyp.6610>, 2008.
- 999 Teuling, A. J. and Troch, P. A.: Improved understanding of soil moisture variability dynamics,  
1000 *Geophysical Research Letters*, 32, <https://doi.org/10.1029/2004GL021935>, 2005.
- 1001 Thieurmél, B. and Elmarhraoui, A.: *suncalc: Compute Sun Position, Sunlight Phases, Moon Position and  
1002 Lunar Phase*, 2022.
- 1003 Tromp-van Meerveld, H. J. and McDonnell, J. J.: On the interrelations between topography, soil depth,  
1004 soil moisture, transpiration rates and species distribution at the hillslope scale, *Advances in Water  
1005 Resources*, 29, 293–310, <https://doi.org/10.1016/j.advwatres.2005.02.016>, 2006.
- 1006 Tsuruta, K., Kwon, H., Law, B. E., and Kume, T.: Relationship between stem diameter and whole-tree  
1007 transpiration across young, mature and old-growth ponderosa pine forests under wet and dry soil  
1008 conditions, *Ecohydrology*, e2572, <https://doi.org/10.1002/eco.2572>, 2023.

- 1009 Vachaud, G., Passerat De Silans, A., Balabanis, P., and Vauclin, M.: Temporal Stability of Spatially  
1010 Measured Soil Water Probability Density Function, *Soil Science Society of America Journal*, 49, 822–  
1011 828, <https://doi.org/10.2136/sssaj1985.03615995004900040006x>, 1985.
- 1012 Van Stan, J. T., Siegert, C. M., Levia, D. F., and Scheick, C. E.: Effects of wind-driven rainfall on  
1013 stemflow generation between codominant tree species with differing crown characteristics, *Agricultural  
1014 and Forest Meteorology*, 151, 1277–1286, <https://doi.org/10.1016/j.agrformet.2011.05.008>, 2011.
- 1015 Van Stan, J. T., Hildebrandt, A., Friesen, J., Metzger, J. C., and Yankine, S. A.: Spatial Variability and  
1016 Temporal Stability of Local Net Precipitation Patterns, in: *Precipitation Partitioning by Vegetation: A  
1017 Global Synthesis*, edited by: Van Stan, I., John T., Gutmann, E., and Friesen, J., Springer International  
1018 Publishing, Cham, 89–104, [https://doi.org/10.1007/978-3-030-29702-2\\_6](https://doi.org/10.1007/978-3-030-29702-2_6), 2020.
- 1019 Vereecken, H., Kamai, T., Harter, T., Kasteel, R., Hopmans, J., and Vanderborght, J.: Explaining soil  
1020 moisture variability as a function of mean soil moisture: A stochastic unsaturated flow perspective,  
1021 *Geophysical Research Letters*, 34, <https://doi.org/10.1029/2007GL031813>, 2007.
- 1022 Vereecken, H., Amelung, W., Bauke, S. L., Bogaen, H., Brüggemann, N., Montzka, C., Vanderborght,  
1023 J., Bechtold, M., Blöschl, G., Carminati, A., Javaux, M., Konings, A. G., Kusche, J., Neuweiler, I., Or,  
1024 D., Steele-Dunne, S., Verhoef, A., Young, M., and Zhang, Y.: Soil hydrology in the Earth system, *Nat  
1025 Rev Earth Environ*, 3, 573–587, <https://doi.org/10.1038/s43017-022-00324-6>, 2022.
- 1026 Vitali, V., Forrester, D. I., and Bauhus, J.: Know Your Neighbours: Drought Response of Norway Spruce,  
1027 Silver Fir and Douglas Fir in Mixed Forests Depends on Species Identity and Diversity of Tree  
1028 Neighbourhoods, *Ecosystems*, 21, 1215–1229, <https://doi.org/10.1007/s10021-017-0214-0>, 2018.
- 1029 Volkmann, T. H. M., Haberer, K., Gessler, A., and Weiler, M.: High-resolution isotope measurements  
1030 resolve rapid ecohydrological dynamics at the soil–plant interface, *New Phytologist*, 210, 839–849,  
1031 <https://doi.org/10.1111/nph.13868>, 2016.
- 1032 Wambsganss, J., Beyer, F., Freschet, G. T., Scherer-Lorenzen, M., and Bauhus, J.: Tree species mixing  
1033 reduces biomass but increases length of absorptive fine roots in European forests, *J Ecol*, 109, 2678–  
1034 2691, <https://doi.org/10.1111/1365-2745.13675>, 2021.
- 1035 Whelan, M. J. and Anderson, J. M.: Modelling spatial patterns of throughfaU and interception loss in a  
1036 Norway spruce (*Picea abies*) plantation at the plot scale, *Journal of Hydrology*, 186, 335–354, 1996.
- 1037 Wiekenkamp, I., Huisman, J. A., Bogaen, H. R., Lin, H. S., and Vereecken, H.: Spatial and temporal  
1038 occurrence of preferential flow in a forested headwater catchment, *Journal of Hydrology*, 534, 139–149,  
1039 <https://doi.org/10.1016/j.jhydrol.2015.12.050>, 2016.

- 1040 Wullaert, H., Pohlert, T., Boy, J., Valarezo, C., and Wilcke, W.: Spatial throughfall heterogeneity in a  
1041 montane rain forest in Ecuador: Extent, temporal stability and drivers, *Journal of Hydrology*, 377, 71–79,  
1042 <https://doi.org/10.1016/j.jhydrol.2009.08.001>, 2009.
- 1043 Yu, K. and D’Odorico, P.: Hydraulic lift as a determinant of tree–grass coexistence on savannas, *New*  
1044 *Phytologist*, 207, 1038–1051, <https://doi.org/10.1111/nph.13431>, 2015.
- 1045 Zacharias, S. and Wessolek, G.: Excluding Organic Matter Content from Pedotransfer Predictors of Soil  
1046 Water Retention, *Soil Science Society of America Journal*, 71, 43–50,  
1047 <https://doi.org/10.2136/sssaj2006.0098>, 2007.
- 1048 Zehe, E., Graeff, T., Morgner, M., Bauer, A., and Bronstert, A.: Plot and field scale soil moisture  
1049 dynamics and subsurface wetness control on runoff generation in a headwater in the Ore Mountains,  
1050 *Hydrol. Earth Syst. Sci.*, 14, 873–889, <https://doi.org/10.5194/hess-14-873-2010>, 2010.
- 1051 Zhang, Y., Wang, X., Hu, R., and Pan, Y.: Throughfall and its spatial variability beneath xerophytic shrub  
1052 canopies within water-limited arid desert ecosystems, *Journal of Hydrology*, 539, 406–416,  
1053 <https://doi.org/10.1016/j.jhydrol.2016.05.051>, 2016.
- 1054 Zhu, X., He, Z., Du, J., Chen, L., Lin, P., and Tian, Q.: Spatial heterogeneity of throughfall and its  
1055 contributions to the variability in near-surface soil water-content in semiarid mountains of China, *Forest*  
1056 *Ecology and Management*, 488, 119008, <https://doi.org/10.1016/j.foreco.2021.119008>, 2021.
- 1057 Zimmermann, A., Zimmermann, B., and Elsenbeer, H.: Rainfall redistribution in a tropical forest: Spatial  
1058 and temporal patterns, *Water Resour. Res.*, 45, <https://doi.org/10.1029/2008WR007470>, 2009.
- 1059 Zuur, A. F., Ieno, E. N., Walker, N., Saveliev, A. A., and Smith, G. M.: Mixed effects models and  
1060 extensions in ecology with R, Springer New York, New York, NY, [https://doi.org/10.1007/978-0-387-](https://doi.org/10.1007/978-0-387-87458-6)  
1061 [87458-6](https://doi.org/10.1007/978-0-387-87458-6), 2009.
- 1062